

Identification of (*R*)-6-(1-(4-Cyano-3-methylphenyl)-5-cyclopentyl-4,5-dihydro-1*H*-pyrazol-3-yl)-2-methoxynicotinic Acid, a Highly Potent and Selective Nonsteroidal Mineralocorticoid Receptor Antagonist

Agustin Casimiro-Garcia,^{*,†} David W. Piotrowski,[‡] Catherine Ambler,[‡] Graciela B. Arhancet,[§] Mary Ellen Banker,[‡] Tereece Banks,[‡] Carine M. Boustany-Kari,[‡] Cuiman Cai,[‡] Xiangyang Chen,[§] Rena Eudy,[‡] David Hepworth,[†] Catherine A. Hulford,[‡] Sandra M. Jennings,[‡] Paula M. Loria,[‡] Marvin J. Meyers,[§] Donna N. Petersen,[‡] Neil K. Raheja,[‡] Matthew Sammons,^{||} Li She,[‡] Kun Song,^{||} Derek Vrieze,[‡] and Liuqing Wei[‡]

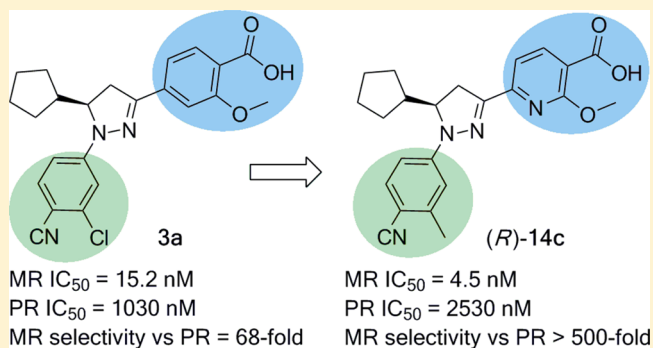
[†]Pfizer Worldwide Research and Development, 200 CambridgePark Drive, Cambridge, Massachusetts 02140, United States

[‡]Pfizer Worldwide Research and Development, Eastern Point Road, Groton, Connecticut 06340, United States

[§]Pfizer Worldwide Medicinal Chemistry, 700 Chesterfield Parkway West, Chesterfield, Missouri 63017, United States

^{||}Pfizer Worldwide Research and Development, 610 Main Street, Cambridge, Massachusetts 02139, United States

ABSTRACT: A novel series of nonsteroidal mineralocorticoid receptor (MR) antagonists identified as part of our strategy to follow up on the clinical candidate PF-03882845 (**2**) is reported. Optimization departed from the previously described pyrazoline **3a** and focused on improving the selectivity for MR versus the progesterone receptor (PR) as an approach to avoid potential sex-hormone-related adverse effects and improving biopharmaceutical properties. From this effort, (*R*)-**14c** was identified as a potent nonsteroidal MR antagonist ($IC_{50} = 4.5$ nM) with higher than 500-fold selectivity versus PR and other related nuclear hormone receptors, with improved solubility as compared to **2** and pharmacokinetic properties suitable for oral administration. (*R*)-**14c** was evaluated in vivo using the increase of urinary Na^+/K^+ ratio in rat as a mechanism biomarker of MR antagonism. Treatment with (*R*)-**14c** by oral administration resulted in significant increases in urinary Na^+/K^+ ratio and demonstrated this novel compound acts as an MR antagonist.



INTRODUCTION

The mineralocorticoid receptor (MR) is a member of the nuclear hormone receptor superfamily (NHRs) and shares structural similarities with other NHRs that also recognize steroidal ligands including progesterone receptor (PR), androgen receptor (AR), glucocorticoid receptor (GR), and estrogen receptor (ER).^{1,2} The steroidal hormone aldosterone is the primary endogenous agonist ligand for MR and mediates sodium reabsorption and potassium excretion in the kidney. Abnormal activation of MR by excessive levels of aldosterone is known to contribute to the development of cardiovascular diseases such as hypertension, congestive heart failure, and chronic kidney disease.^{3,4} Overactivation of MR in the kidney and other tissues has also been associated with the development of fibrosis, inflammation, and oxidative stress.^{5,6} Thus, intervention with MR antagonists represents an attractive therapeutic option for the treatment of these conditions. It is also important to note that recent progress has been made in

the identification of potent and selective inhibitors of aldosterone synthase,⁷ the crucial enzyme in the biosynthesis of aldosterone, providing another therapeutic approach for the treatment of aldosterone related cardiovascular and renal diseases. There are two steroidal MR antagonists currently in use, spironolactone and eplerenone (Figure 1). These agents have been proven to reduce the risk of death and hospitalization in three large randomized clinical trials in patients with severe heart failure.^{8–10} Clinical studies in smaller patient populations have shown that steroidal MR antagonists also provide benefits with respect to blood pressure (BP) control and antiproteinuric effects in diabetic nephropathy.^{11–14} However, therapeutic use of these agents has been limited by their side effects. Among them are the sex hormone related adverse effects such as impotence, gynecomastia, and menstrual

Received: February 7, 2014

Published: April 16, 2014

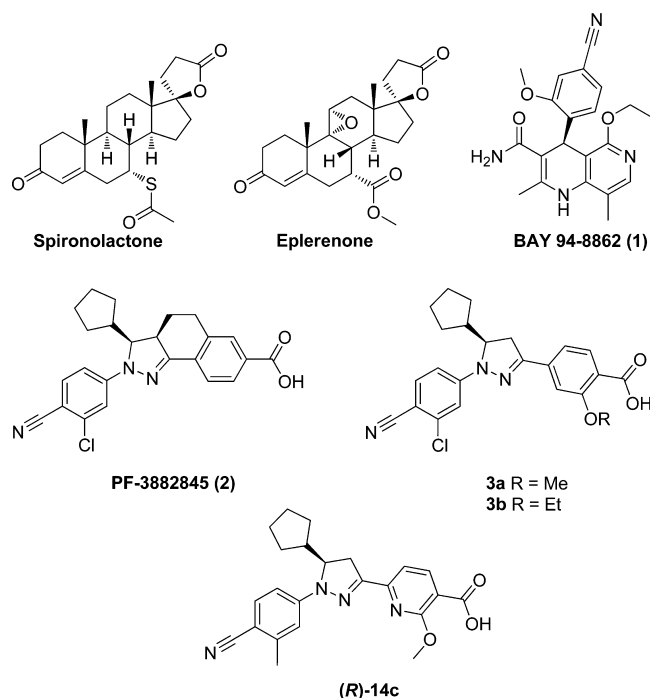


Figure 1. Marketed steroid MR antagonists and selected non-steroidal MR antagonists.

irregularities observed with spironolactone therapy. These undesired actions are likely explained by the lack of selectivity of spironolactone for the mineralocorticoid receptor over androgen receptor and progesterone receptor. Eplerenone has an improved selectivity profile compared to spironolactone, leading to negligible sex hormone adverse effects but also a significantly less potent agent.¹⁵ Another well-known side effect of steroid MR antagonists is hyperkalemia that can cause cardiac dysfunction and even lead to sudden death.¹⁶

In recent years, there have been new efforts to overcome the limitations of the steroid MR antagonists with the discovery of potent, selective, and safer nonsteroidal compounds.¹⁷ Among this novel class, BAY 94-8862 (**1**, Figure 1) is the most advanced nonsteroidal MR antagonist investigated in clinical trials.¹⁸ The first phase II study was recently published and showed highly encouraging results.¹⁹ Treatment with **1** was associated with a remarkable reduction of hyperkalemia and worsening renal function as compared to spironolactone treatment. In addition, biomarker data suggests that the lower incidence of side effects most probably does not come at a cost of lower efficacy. Differences in tissue distribution may in part explain the reduction of hyperkalemia observed with this novel agent. While **1** distributed equally to kidney and heart in rats,¹⁹ spironolactone had at least 6-fold higher renal concentration than cardiac tissue concentration.^{20,21} These results suggest that, at least in rats, the steroid MR antagonist spironolactone reached higher local kidney concentrations that may produce increased renal effects when compared to respective cardiac effects.²¹ The more equal distribution between renal and cardiac tissue of **1** may explain the reduction of the incidence of hyperkalemia and renal adverse events reported with this agent when compared to spironolactone in the phase II study.¹⁹ Collectively, these highly encouraging results support the search for novel nonsteroidal MR antagonists with improved profiles.

As part of our discovery efforts to identify novel nonsteroidal MR antagonists,^{22–28} our group recently reported the discovery of a new class of nonsteroidal MR antagonists based on a pyrazoline scaffold.²⁹ Conformational restriction of this template led to the identification of **2**³⁰ as a potent nonsteroidal MR antagonist (MR binding IC_{50} = 9 nM; MR functional IC_{50} = 21 nM) with favorable pharmacokinetic profile and selectivity over related steroid receptors (PR, 46-fold selectivity; GR, AR, ER, >900-fold selectivity). Evaluation of **2** in the Dahl salt sensitive rat, a preclinical model of salt induced hypertension and nephropathy, showed a striking reduction of blood pressure, improved kidney protection, and decreased urinary albumin excretion than that observed in the eplerenone group.²⁹ Furthermore, measurement of serum potassium levels suggested that **2** may have a reduced risk of hyperkalemia relative to eplerenone. Utilizing a rat model of aldosterone-induced renal damage, the effect of **2** and eplerenone for prevention of increases in urinary albumin to creatinine ratio (UACR) and for elevation of serum potassium was established.³¹ Data from these studies indicated that **2** has a larger therapeutic index, calculated as the ratio of the EC_{50} for increasing serum potassium to the EC_{50} for UACR lowering, than eplerenone. Thus, pyrazoline **2** may present significantly lower risk for hyperkalemia compared to eplerenone. On the basis of its robust in vitro profile, efficacy, pharmacokinetic, and safety profile, **2** was advanced to clinical trials.

Our strategy to further build upon this novel class of nonsteroidal MR antagonists focused on two specific areas. First, selectivity over the steroid receptor PR was identified as an area with room for improvement. Thus, to minimize the potential for sex hormone related side effects, identification of novel nonsteroidal MR antagonists with >100-fold selectivity over PR was envisioned as an important goal for follow-up compounds. The second goal was to drive toward improved biopharmaceutical properties. The conformationally constrained pyrazolines are characterized as a moderately lipophilic carboxylic acid series (**2**: measured Log D = 3.5) with relatively low solubility (**2**: solubility in 20 mM potassium phosphate buffer at pH 6.3 = 1 μ g/mL; solubility in fasted state simulated intestinal fluid (FaSSIF) at pH 6.8 = 81 μ g/mL). The low solubility may preclude the ability to dose solution formulations of this class of compounds in the clinic without the utilization of more complex formulation technologies for development.³² Hence, to circumvent these potential limitations, a second goal for follow-up candidates was to drive toward higher solubility by improving physicochemical properties, in particular reduction of lipophilicity and molecular weight. Our plan to follow up on the clinical candidate was centered on a series of nonconformationally restricted pyrazoline analogues possessing high potency, favorable selectivity, and pharmacokinetic properties that were identified along with the discovery of **2**. Among them, pyrazoline **3a** represents an example that exhibits these attributes.²⁹ As further elaborated later, the unexpected discovery that replacement of the 3-chloro-4-cyanophenyl ring in this series with a 4-cyano-3-methylphenyl group afforded significant improvement in the selectivity versus PR provided additional guidance to optimize this series. In this report, the description of the elaboration of this series of nonconformationally restricted pyrazolines into a potent class of nonsteroidal MR antagonists with unprecedented selectivity versus related steroid hormone receptors and the identification (R)-6-(1-(4-cyano-3-methylphenyl)-5-cyclopentyl-4,5-dihydro-1H-pyrazol-

3-yl)-2-methoxynicotinic acid ((*R*)-14c) as a preclinical candidate to progress into further studies are presented.

RESULTS AND DISCUSSION

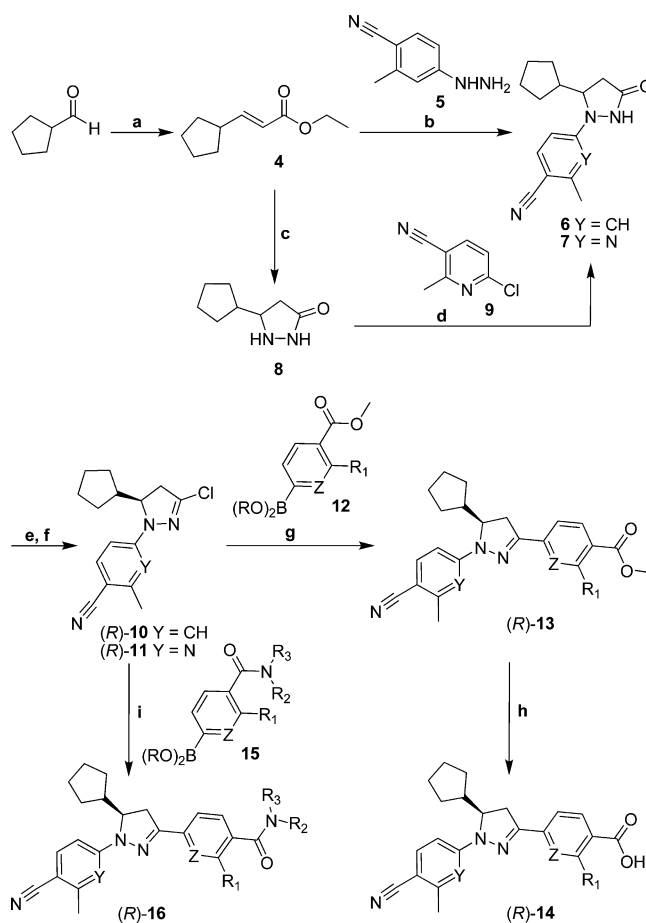
Our plan to improve the physicochemical properties, with an ultimate goal of achieving higher solubility, focused on decreasing lipophilicity and molecular weight in this series. Modifications of the aromatic rings were planned to pursue these objectives and included: (a) incorporation of nitrogen at the benzoic acid ring, (b) replacement of the 3-chloro-4-cyanophenyl ring in 3a with other more polar and/or lower molecular weight cyanophenyl or cyanoheteroaryl rings, and (c) replacement of the cyclopentyl ring at C-5 of the pyrazoline ring with smaller and less lipophilic groups. Along with changes in physicochemical properties derived from these modifications, selected groups among this set were also identified that provided significant improvement in selectivity for MR versus PR, addressing in this manner our second goal.

The main route for the preparation of the new compounds consisted of Suzuki cross-coupling of chiral chloropyrazolines (*R*)-10 and (*R*)-11 with appropriate boronate or boronic acids 12 or 15 as described in Scheme 1. The preparation of chloropyrazolines (*R*)-10 and (*R*)-11 was carried out employing a route similar to those previously described.²⁹ Briefly, condensation of cyclopentanecarboxaldehyde with ethyl 2-(diethoxyphosphoryl)acetate gave unsaturated ester 4, which was reacted with hydrazine 5 under basic conditions to provide pyrazolinone 6. For the preparation of pyrazolinone 7, α,β -unsaturated ester 4 was first reacted with hydrazine hydrate in refluxing ethanol to provide 8. Displacement of chloride from 9 with 8 under microwave conditions afforded pyrazolinone 7. Treatment of pyrazolinones 6 or 7 with phosphorus oxychloride gave racemic chloropyrazolines. Resolution of these intermediates by chiral supercritical fluid chromatography (SFC) conditions afforded enantiomerically pure pyrazolines (*R*)-10 and (*R*)-11. Suzuki coupling of (*R*)-10 or (*R*)-11 with an appropriate boronate or boronic acid 12 afforded the corresponding aryl esters (*R*)-13. Hydrolysis under basic conditions gave enantiopure pyrazoline carboxylic acids (*R*)-14. Our efforts to optimize the Suzuki cross-coupling with the highly substituted 2-pyridylboronate 12c and its application for the large scale preparation of (*R*)-14c shown in Scheme 2 have been reported.³³ The opposite enantiomer (*S*)-14c was prepared using an earlier route that was previously discussed to afford racemic 14c.³³ Chiral SFC separation of racemic 14c provided (*S*)-14c. Suzuki cross-coupling was also utilized to prepare analogues (*R*)-16 in a single step from chloropyrazolines (*R*)-10 or (*R*)-11 and boronates 15.

The condensation route depicted in Scheme 3 was utilized for the preparation of (*R*)-19. This route consists of the condensation of the α,β -unsaturated ketone 17 with hydrazine 18 in the presence of sodium ethoxide in ethanol to give the racemic nicotinic acid derivative. Chiral SFC separation of racemic acid provided enantiopure (*R*)-19.

The preparation of (*R*)-25 is described in Scheme 4 and follows a similar route to that described for analogues (*R*)-14 and (*R*)-16. It departs from the condensation of α,β -unsaturated ester 20 and hydrazine 21, the latter obtained from the reaction of chloropyridine 8 with hydrazine hydrate. Pyrazolinone 22 obtained in this manner was then reacted with phosphorus oxychloride to give racemic chloropyrazoline 23. Suzuki coupling of 23 with boronate 12c afforded the corresponding ester 24. Hydrolysis under basic conditions,

Scheme 1. Synthesis of Pyrazoline Derivatives (*R*)-14 and (*R*)-16 via Suzuki Cross-Coupling^a

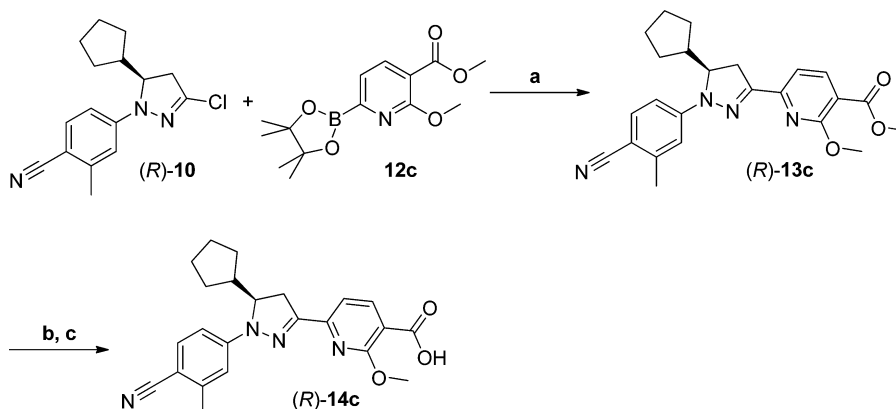


^aReagents and conditions: (a) (EtO)₂POCH₂CO₂Et, NaOEt, 83%; (b) 5, NaOEt, 79%; (c) NH₂NH₂, EtOH/H₂O, reflux, 48 h, 63%; (d) 8, H₂O, microwaves, 150 °C, 0.5 h, 87%; (e) POCl₃, CH₃CN, 80 °C, 79–89%; (f) chiral SFC; (g) 12, Pd(PPh₃)₄, 2 M Na₂CO₃, DME, 80 °C; (h) LiOH, THF/H₂O, then HCl/H₂O; (i) 15, Pd(PPh₃)₄, 2 M Na₂CO₃, DME, 80 °C.

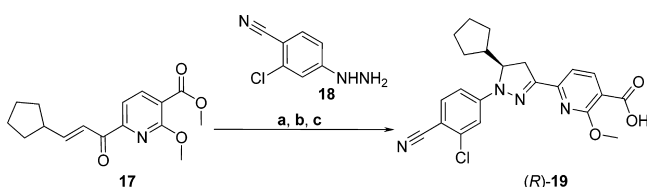
followed by chiral SFC separation, gave enantiopure (*R*)-25. The assignment of the stereochemistry for (*R*)-25 was based on its biological activity and the precedented higher functional activity and potency to MR of the *R*-enantiomer among pairs of enantiomers of pyrazoline analogues in both previous and current work (compare (*R*)-14c vs (*S*)-14c).²⁹

A number of amides 16, acylsulfonamides 26, and acyl aminotetrazole 27 analogues were prepared from appropriate carboxylic acids 14 under the conditions described in Scheme 5.

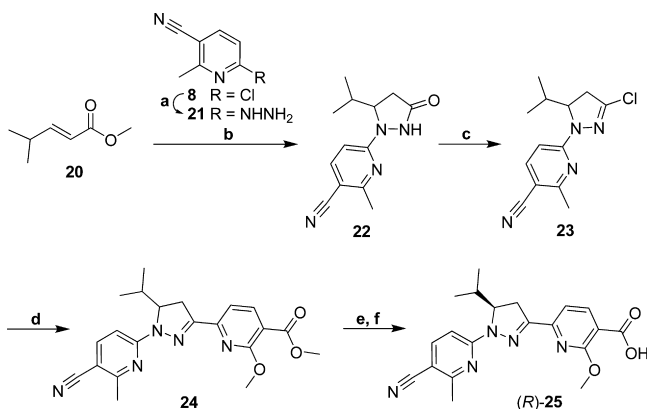
The new pyrazoline analogues were first evaluated in a functional Gal4-based cellular assay to assess the transcriptional activity of MR antagonists and the IC₅₀ values are summarized in Tables 1 and 2. New compounds were also tested simultaneously in a panel of cell-based reporter assays that measured the transcriptional activity of new compounds over related steroid hormone receptors including PR, GR, and AR. The IC₅₀ values derived from these assays are also included in Tables 1 and 2. Eplerenone, 2, 3a, and 3b are included in Table 1 as reference compounds. As one of the goals of this work was to improve solubility by reduction of lipophilicity and MW, experimental Log *D* was determined for the majority of the new compounds using the octanol/buffer shake flask method. A

Scheme 2. Optimized Suzuki Cross-Coupling Conditions for the Large Scale Preparation of (R)-14c^a

^aReagents and conditions: (a) Pd₂(dba)₃, X-Phos, 1 M K₂CO₃, THF, 65 °C, 85%; (b) 1 N NaOH, THF, 40 °C; (c) EtOH/H₂O slurry, 95% (2-steps)

Scheme 3. Synthesis of (R)-19 via Condensation Route^a

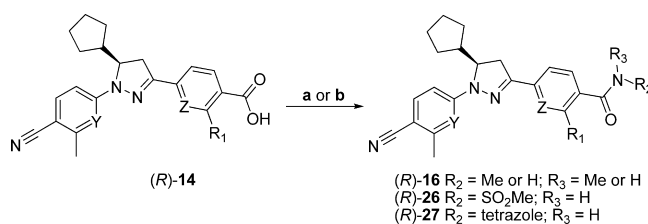
^aReagents and conditions: (a) 18, NaOEt, 50 °C; (b) aqueous HCl, 42% (2 steps); (c) chiral SFC.

Scheme 4. Synthesis of Pyrazoline Analogue (R)-25^a

^aReagents and conditions: (a) hydrazine hydrate, EtOH, 80 °C, 100%; (b) KOtBu, EtOH, 80 °C, 28%; (c) POCl₃, CH₃CN, 80 °C, 46%; (d) 12c, Pd(PPh₃)₄, 2 M Na₂CO₃, DME, 80 °C, 45%; (e) LiOH, THF/H₂O, then HCl/H₂O, 85%; (f) chiral SFC.

high-throughput kinetic solubility assay measured in 100 mM potassium phosphate buffer at pH 6.5 was utilized to follow solubility improvements. Additional solubility determinations were performed with selected compounds. Experimental Log *D* and solubility values are included in Tables 1 and 2.

Pyrazoline 3a represented an interesting lead to start our efforts aimed at increased selectivity versus PR and improved solubility through reduction of lipophilicity and MW. This compound combined good MR potency (IC₅₀ = 15 nM), slightly higher selectivity versus PR when compared to 2 (2, 45-fold, versus 3a, 67-fold) and retained high selectivity over GR and AR.²⁹ The higher selectivity for PR in this noncyclic

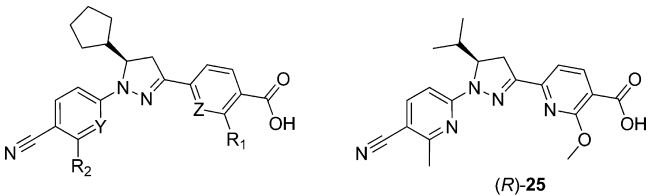
Scheme 5. Synthesis of Pyrazoline Analogues (R)-16–(R)-27^a

^aReagents and conditions: (a) (i) CDI, (ii) amine, DMF-THF, rt, 12 h; (b) MeSO₂NH₂, DIEA, HATU, DCM, rt, 16 h.

pyrazoline series was also observed in the closely related ethoxy ether 3b that exhibited a 78-fold selectivity versus PR. Pyrazoline 3a is also a more polar compound with a Log *D* value that is more than one log unit lower than 2 (3a, Log *D* = 2.1; 2, Log *D* = 3.5). This reduction in lipophilicity is likely reflected in the 2-fold increase in solubility observed with 3a (3a, solubility = 271 μM; 2, solubility = 131 μM). Thus, on the basis of the combined profile of 3a, we focused our efforts on modifications around this interesting lead. Replacement of the 3-chloro-4-cyanophenyl ring in 3a with a 4-cyano-3-methylphenyl group was investigated to decrease MW, while it was expected that this modification would retain similar MR potency. Two compounds were prepared initially to understand the impact of this transformation (R)-14a and (R)-14b. In both compounds, the combination of a small improvement in MR potency and decrease in PR activity led to higher selectivity versus PR ((R)-14a, 301-fold; (R)-14b, 204-fold) when compared to 3a. As it will be further elaborated later, the observed improvement in selectivity versus PR with the 4-cyano-3-methylphenyl group was not only demonstrated in these initial analogues but was exhibited in several additional compounds. Higher solubility was observed in (R)-14a (solubility = 305 μM) when compared to 2 that likely resulted from a reduction in lipophilicity (Log *D* = 2.2).

Incorporation of nitrogen in the aromatic ring displaying the carboxylic acid was utilized to decrease lipophilicity. Derivatives of 2-alkoxynicotinic acid were prepared that led to remarkable improvements in the selectivity versus PR. Combination of 2-methoxynicotinic acid or 2-ethoxynicotinic acid groups with the 4-cyano-3-methylphenyl group led to highly potent MR

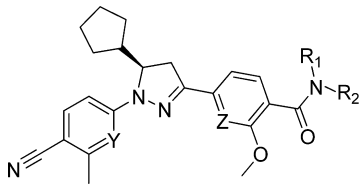
Table 1. Antagonistic Activity of New Pyrazoline Analogues (R)-14, (R)-19, and (R)-25 in MR and Related Steroid Hormone Receptors



compd	R ₁	R ₂	Y	Z	IC ₅₀ (nM) ^a				Log D ^b	solubility ^c (μM)
					MR	PR	GR	AR		
eplerenone					122					
2					9.2	416	>10000	>8910	3.5	131
3a	OCH ₃	Cl	CH	CH	15.2	1030	>10000	>10000	2.1	271
3b	OCH ₂ CH ₃	Cl	CH	CH	25.6	2010	>10000	>10000	2.6 ^d	34
R-14a	OCH ₃	CH ₃	CH	CH	9	2720	>10000	>10000	2.2	305
R-14b	OCH ₂ CH ₃	CH ₃	CH	CH	10.7	2190	>10000	>10000	2.7	193
R-14c	OCH ₃	CH ₃	CH	N	4.5	2530	>10000	>10000	2.2	312
S-14c	OCH ₃	CH ₃	CH	N	4450	ND ^e	ND	ND	2.2	338
R-14d	OCH ₃	CH ₃	N	N	7.6	1590	6800	9050	2.0	324
R-14e	OCH ₃	CH ₃	N	CH	18	6810	ND	>10000	1.7	308
R-14f	H	CH ₃	N	CH	21.4	5310	ND	>10000	2.6	106
R-14g	OCH ₂ CH ₃	CH ₃	CH	N	4.4	2600	>10000	>10000	3.0	138
R-19	OCH ₃	Cl	CH	N	55.9	806	>10000	>10000	2.3	284
R-25					30.7	2040	ND	ND	1.6	803

^aFunctional Gal4-based cellular assay; mean value of at least two determinations. ^bExperimental Log D determined using octanol/buffer shake flask method. ^cKinetic solubility was determined as previously described.³⁴ ^dCalculated Log D value. ^eNot determined.

Table 2. Antagonistic Activity of New Pyrazoline Analogues (R)-16, (R)-26, and (R)-27 in MR and Related Steroid Hormone Receptors



compd	R ₁	R ₂	Y	Z	IC ₅₀ (nM) ^a				Log D ^b	solubility ^c (μM)
					MR	PR	GR	AR		
3a					9	2720	>10000	>10000	2.1	271
3b					10.7	2680	>10000	>10000	2.6 ^d	34
R-14c			CH	N	4.5	2530	>10000	>10000	2.2	312
R-16a	H	H	CH	N	2.7	494	2770	3250	3.8	<25
R-16b	CH ₃	H	CH	N	17.8	3670	ND ^e	>10000	4.4 ^d	<25
R-16c	CH ₃	CH ₃	CH	N	3.7	1490	ND	>10000	3.5	<25
R-16d	H	H	N	N	4.3	597	4800	7780	3.4	<25
R-16e	CH ₃	H	N	N	3.3	550	ND	8520	3.2	50
R-16f	CH ₃	CH ₃	N	N	9.4	1520	ND	>10000	4.1	<25
R-26a	SO ₂ Me	H	CH	N	2.8	2480	>10000	>10000	2.3	239
R-26b	SO ₂ Me	H	N	N	4.1	831	ND	9940	1.9	39
R-27	tetrazole	H	CH	N	2.2	684	ND	>10000	3.2	<25

^aFunctional Gal4-based cellular assay; mean value of at least two determinations. ^bExperimental Log D determined using octanol/buffer shake flask method. ^cKinetic solubility was determined as previously described.³⁴ ^dCalculated Log D value. ^eNot determined.

antagonists (R)-14c and (R)-14g with MR IC₅₀ values of 4.5 and 4.4 nM, respectively, that represents an approximately 3-fold potency gain when compared to 3a. This improvement in MR potency was accompanied by lower PR activity in both compounds ((R)-14c, PR = 2530 nM; (R)-14g, PR = 2600 nM), leading to unprecedented selectivity versus PR of greater than 500-fold in both analogues. Interestingly, (R)-14c was

about as polar as 3a, with a Log D value of 2.2, and exhibited solubility of 312 μM that represented a 2-fold enhancement versus 2. The lipophilicity and solubility of the ethoxy ether (R)-14g were in a similar range as those observed with 2, and thus additional ethoxy ether analogues were not pursued further as they were not expected to address the solubility goal of this work. Combination of 2-methoxynicotinic acid with 3-

chloro-4-cyanophenyl provided (R)-19 that showed a significant loss of MR potency ($IC_{50} = 55.9$ nM) and a gain in PR activity (PR = 806 nM) when compared to (R)-14c. It is important to notice that these two compounds ((R)-19 vs (R)-14c) only differ by the substituent at the ortho position on the cyanophenyl ring (Cl vs CH_3). A similar trend was observed between 3a and (R)-14a for PR activity, but only a 2-fold difference for MR activity was obtained. Taken together, these results suggest that in going from chlorine to methyl at the C-3 position of the cyanoaryl ring there is an enhancement in MR potency and reduction in PR activity. These results might be explained by electron density differences of the nitrile derived from variations at C-3 of the cyanoaryl moiety that alter the hydrogen-bonding capacity of this group. These results also suggest that the combination of the 2-methoxynicotinic acid with the 4-cyano-3-methylphenyl group provides highly optimized interactions with MR, as well as reduced binding to PR, leading to the desired profile in terms of potency and selectivity.

In an effort to further investigate the effect of reduction of lipophilicity in this series, the set of analogues (R)-14d–f were prepared by incorporating the more polar 2-methylnicotinonitrile combined with selected benzoic acid or nicotinic acid groups. The combination of 2-methylnicotinonitrile with 2-methoxynicotinic acid gave (R)-14d that showed potent MR activity ($IC_{50} = 7.6$ nM) and higher than 200-fold selectivity versus PR. It is interesting to notice that the incorporation of nitrogen in the cyanoaryl ring did not change noticeably the lipophilicity and solubility in (R)-14d (Log $D = 2.0$; solubility = 324 μ M) when compared to (R)-14c. By combining 2-methylnicotinonitrile with 2-methoxybenzoic acid, (R)-14e was obtained. This compound showed good MR potency ($IC_{50} = 18$ nM) and low PR activity ($IC_{50} = 6810$ nM) that resulted in higher than 300-fold selectivity for MR. Interestingly, removing the methoxy substituent from (R)-14e to give (R)-14f was tolerated, and the latter compound showed higher than 200-fold selectivity versus PR. However, this transformation also led to an increase in lipophilicity and reduction of solubility ((R)-14e, Log $D = 1.7$; solubility = 308 μ M vs (R)-14f, Log $D = 2.6$; solubility = 106 μ M) and was not pursued further.

The cyclopentyl ring was previously established as the optimal C-5 substituent on the pyrazoline ring.²⁹ However, our interest to investigate additional reduction of lipophilicity in the current series led us to consider smaller, less lipophilic groups at this position. A C-5 isopropyl group was previously examined in this series and led to about 7-fold reduction in MR potency. However, this group represented an interesting option to increase polarity and solubility. With this knowledge in hand, (R)-25 was prepared. Pairwise comparison of (R)-25 versus (R)-14d, differing only in the C-5 substituent (isopropyl vs cyclopentyl), showed that the smaller isopropyl group led to a 4-fold reduction in MR potency ((R)-25, $IC_{50} = 30.7$ nM, vs (R)-14d: $IC_{50} = 7.6$ nM) and about similar PR activity. These effects resulted in lower selectivity versus PR (66-fold). As expected, the incorporation of the C-5 isopropyl group led to a more polar compound (Log $D = 1.6$) with higher solubility (803 μ M). While it is expected that the MR potency can be improved by replacing the 2-methylnicotinonitrile group in (R)-25 with the 4-cyano-3-methylphenyl moiety, the lack of more significant reduction of PR activity with the C-5 isopropyl group was not encouraging enough to pursue additional analogues.

The remarkable selectivity versus PR observed with several carboxylic acid analogues described above represented a significant advancement in the optimization of this series of nonsteroidal MR antagonists and far exceeded our initial goal. It was intriguing to consider if this unprecedented level of selectivity was a property exclusively exhibited by carboxylic acid derivatives, or if it would be retained in analogues possessing other functionality. To address this question, several amides were proposed. A set of amides derived from the highly potent and selective carboxylic acid (R)-14c was prepared to give (R)-16a–c. The replacement of the carboxylic acid in (R)-14c with the primary amide in (R)-16a led to approximately similar MR potency ($IC_{50} = 2.7$ nM), but this was accompanied by augmented PR activity that resulted in lower selectivity versus PR (185-fold). The *N*-methyl amide (R)-16b showed an approximately 4-fold drop in MR potency ($IC_{50} = 17.8$ nM) when compared to the carboxylic acid. The *N,N*-dimethyl amide (R)-16c was the most interesting compound from this set and combined potent MR activity ($IC_{50} = 3.7$ nM) and high selectivity versus PR (405-fold). The selectivity observed with (R)-16c was remarkable and suggested further evaluation to determine if this trend would be observed with additional amides and other analogues possessing different functionality. A set of additional amides derived from carboxylic acid (R)-14d were prepared and provided (R)-16d–f. The set of amides (R)-16d–f showed that in general there is not a significant increase in selectivity with this functionality as compared to the carboxylic acid. This is exemplified with the *N*-methyl amide (R)-16e that, despite showing potent MR activity ($IC_{50} = 3.3$ nM), its selectivity versus PR (166-fold) was slightly lower than that observed with carboxylic acid (R)-14d. It is important to note that in going from the carboxylic acid to the neutral amides (R)-16a–f a significant erosion of solubility (<25 to 50 μ M) was observed that is highly likely associated with an increase in lipophilicity as assessed from higher Log D values (Log D 3.2–4.4).

An interesting question that was not addressed with the amides was whether an acidic functionality is required in this series to achieve high selectivity over PR. A set of carboxylic acid bioisosteres, including acylsulfonamide (R)-26a and (R)-26b and acyl tetrazole (R)-27 derived from (R)-14c or (R)-14d, was prepared to investigate if other acidic compounds can indeed provide high selectivity. The results obtained with these compounds are interesting. All three compounds exhibited potent MR activity ((R)-26a, $IC_{50} = 2.8$ nM; (R)-26b, $IC_{50} = 4.1$ nM; (R)-27, $IC_{50} = 2.2$ nM). In the case of acylsulfonamides (R)-26a, the potent MR activity was combined with no increase in PR activity when compared to the carboxylic acid, and this led to a superb, higher than 800-fold selectivity versus PR. Acylsulfonamides (R)-26b showed similar selectivity versus PR (203-fold) to that of the corresponding acid. The acyl tetrazole (R)-27 was also highly selective versus PR (304-fold). The results obtained with the compounds possessing an acid functionality in this series, including carboxylic acid, acylsulfonamide, and acyl tetrazole, support that an acidic group contributes to the high selectivity versus PR. However, this is not a unique feature of the acidic compounds, as selected amides also displayed higher than 400-fold selectivity versus PR.

The results from this work demonstrated that the scaffold obtained with (R)-14c is highly favorable to achieve high potency for MR and high selectivity versus PR. It is important to note that while this series was optimized, efforts to

rationalize the binding of this scaffold to MR and its exquisite selectivity through docking experiments, in lieu of X-ray crystallography data, did not provide satisfactory results capable of fully explaining the observed SAR. The previously described induced-fit model that was invoked to describe the binding of **2** to MR did not appear capable of explaining SAR observed in the nonconformational restricted pyrazoline analogues reported in this work.²⁹ In particular, limitations were found to correctly characterize the interactions of neutral analogues like the amides described above. The identification of (R)-**14c** and its high MR potency and selectivity over related nuclear hormone receptors was an empirical finding. Optimization efforts were mostly driven through experimental observations rather than structure-guided design.

The disclosure of the first crystal structures of nonsteroidal MR antagonists bound to the ligand binding domain (LBD) of MR by the Takeda group has provided highly valuable knowledge about the mode of interaction of this class of MR antagonists.^{35,36} It also provided a new opportunity to develop a docking model of (R)-**14c** bound to MR using this new information. The proposed binding mode of (R)-**14c** to the ligand binding domain of MR was created in a two-step process. The initial binding pose was generated by docking using GLIDE program with the rigid protein structure.^{37–39} For the docking experiment, the protein structure was built using the X-ray crystal structure of human MR ligand-binding domain bound to a nonsteroidal antagonist (PDB ID: 3VHV).³⁵ Several X-ray crystal structures of MR have been reported.^{35,36,40–43} One interesting difference among these structures is the side chain conformation of Met852 from H7 helix. In the case of steroidal ligands, it adopts an extended conformation when the bound ligand does not display an angular group, like in the case of corticosterone (PDB ID: 3A3I),⁴¹ but it adopts a folded-back conformation when the bound steroid has an angular substituent like in the case of spironolactone with its C-7 thioacetyl group (PDB ID: 3VHU),³⁵ creating a small lipophilic pocket for positioning of this group. Because (R)-**14c** contains an angular cyclopentyl group, the X-ray structure 3VHV was selected, in which the side chain of Met852 is folded-back and additional hydrophobic space is created. In the second step, the protein–ligand complex went through minimization and equilibration, then 1 ns molecular dynamic simulation to optimize the protein–ligand interaction. The conformation with lowest energy was selected as the proposed binding mode.

The final binding pose of (R)-**14c** is depicted in Figure 2. The biggest difference between the X-ray structure 3VHV and the new protein conformation after MD simulation is the side chain rotation of Phe941. The χ_1 angle is changed from 179° to –45°. The proposed binding model is highly consistent with the expected mode of interaction of MR antagonists. The cyano group of (R)-**14c** engages in H-bonding with Gln776 from H3 helix and Arg817 from H5 helix of MR to mimic the interactions of the 3-keto group on the steroids. The cyclopentyl ring occupies the pocket created by the folded-back conformation of Met852 and, as referred above, occupied by the C-7 thioacetyl group in the spironolactone crystal structure.⁴³ This pocket is lined by several lipophilic residues including Leu, Met, Cys, and Phe and capable of accommodating a variety of angular lipophilic groups at C-5 of the pyrazoline scaffold. This makes the proposed model consistent with previous SAR observed in the nonconformationally restricted pyrazoline series.²⁹ The carboxylic acid of (R)-**14c** engages in H-bonding with Thr945 from H11 helix and mimics

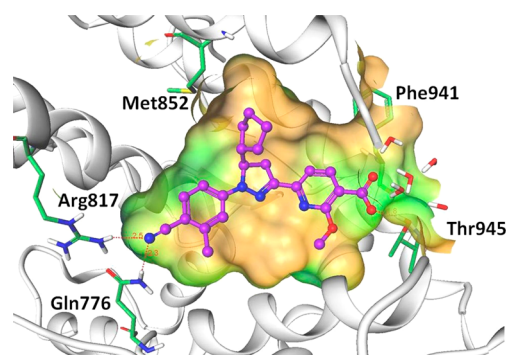


Figure 2. Proposed binding mode of (R)-**14c** (magenta) to the ligand binding domain of MR (white α -helices with key residues in green). The nitrile group of (R)-**14c** is engaged in H-bonding to Arg817 and Gln776. The carboxylate group interacts with Thr945 through H-bonding interactions. The cyclopentyl group occupies a lipophilic groove created by the folded-back conformation of Met852.

the interaction of the hydrophilic group displayed in D-ring of the steroid.

Docking experiments were also carried out to determine if analogues containing functionality other than the carboxylic acid would be predicted to achieve similar interactions using the proposed binding model. Satisfactorily, docking of amide (R)-**16a** and acylsulfonamide (R)-**26a** showed both compounds with docking scores (–9.5 and –9.3, respectively) that were similar to the one obtained for the carboxylic acid (R)-**14c** (docking score = –9.7). Both compounds bound to MR in a similar mode as observed with (R)-**14c**. In the case of (R)-**16a** and (R)-**26a**, the carbonyl group from the nicotinic acid group is still able to make H-bonding with Thr945. These results are consistent with the observed SAR and further validated the proposed binding model.

The carboxylic acid (R)-**14c** and acylsulfonamide (R)-**26a** differentiated from other compounds by the potent MR activity, higher than 500-fold selectivity versus PR, and increased polarity and solubility. Further evaluation of these compounds showed that (R)-**26a** exhibited high in vitro human liver microsomes intrinsic clearance (Cl_{int} = 175 μ L/min/mg), while (R)-**14c** showed low intrinsic clearance in this assay (Cl_{int} < 14 μ L/min/mg). These results led to focus additional characterization efforts on (R)-**14c**. This compound was profiled in both functional and binding assays across a panel of NHRs, including MR, PR, GR, AR, and ER α (Table 3). Pyrazoline (R)-**14c** demonstrated high potency in both functional and binding MR assays, with strong correlation between both screens. The higher than 500-fold selectivity

Table 3. Evaluation of (R)-**14c** across a Panel of NHRs

assay	(R)- 14c
MR binding $IC_{50} \pm SD$ (nM) ^a	1.8 \pm 1.4
MR functional $IC_{50} \pm SD$ (nM) ^a	4.5 \pm 2.3
PR binding $IC_{50} \pm SD$ (nM) ^b	3908 \pm 839
PR functional $IC_{50} \pm SD$ (nM) ^a	2529 \pm 980
GR binding $IC_{50} \pm SD$ (nM) ^b	>9497 \pm 803
GR functional IC_{50} (nM) ^b	>10000
AR functional IC_{50} (nM) ^b	>10000
ER α binding IC_{50} (nM) ^c	>10000

^aMean value of more than 10 experiments. ^bMean value of at least three experiments. ^cMean value of two experiments.

versus PR determined in the functional assay was also fully demonstrated in the binding assay. Similarly, GR and ER α binding assay results further demonstrated the high selectivity of (R)-14c over these NHRs. The solubility of this compound was determined under different conditions using crystalline material. These screens were done as thermodynamic equilibrium solubility measurements. In phosphate buffer, (R)-14c showed a solubility of 0.19 mg/mL, while its solubility in fasted state simulated intestinal fluid (FaSSIF) was determined to be 0.58 mg/mL. In both measurements, (R)-14c demonstrated a robust improvement in solubility (>7-fold) as compared to the solubility of 2 under similar conditions, accomplishing in this way one of the goals of this work. As the next steps in the characterization of this compound was to perform studies in rat, the pharmacokinetic properties of (R)-14c were evaluated in this species to determine its suitability for oral administration (Table 4). In vivo clearance was about half

Table 4. Pharmacokinetic Properties of (R)-14c in Rat

route	dose (mg/kg)	AUC (ng·h/mL)	$t_{1/2}$ (h)	F (%)	Cl (mL/min/kg)	V_{ss} (L/kg)
IV	1	494	2.3		33	3.1
PO	5	1320		54		

hepatic blood flow (Cl = 33 mL/min/kg) with a moderate volume of distribution (V_{ss} = 3.1 L/kg). The measured half-life was 2.3 h. Bioavailability was moderate (54%) following a 5 mg/kg dose. The profile of this compound was considered appropriate to progress into in vivo studies.

Our group recently reported the validation of the use of urinary sodium to potassium (Na^+/K^+) ratio in rat as a quantitative mechanism biomarker of MR antagonism.⁴⁴ In this study, the functional in vitro IC_{50} value for eplerenone was found to be close (5-fold) to the EC_{50} value derived from its effect on increasing urinary Na^+/K^+ ratio in rat. In addition, the EC_{50} value generated from its effect on urinary Na^+/K^+ ratio in healthy volunteers was also found to be near (2-fold) to the EC_{50} value generated in rat. The cyclic pyrazoline 2 was also assessed in this study, and its potency for increasing urinary Na^+/K^+ ratio in rat was also determined to be close to its functional in vitro IC_{50} value. These results established the rat-to-human translatability of the urinary Na^+/K^+ ratio as a mechanism biomarker of MR antagonism. In the current study, this method was utilized to evaluate the effects of MR antagonism with the novel pyrazoline (R)-14c. Briefly, following acclimation, animals were randomly assigned to treatment groups ($n = 6/\text{group}$) to receive a single oral dose of 3, 10, or 30 mg/kg (R)-14c or vehicle or 30 mg/kg eplerenone used as a positive control. Urine samples were collected overnight prior to dosing and at intervals of 0–2, 2–4, and 4–7 h postdose for measurement of urinary sodium and potassium concentration. As observed with the positive control eplerenone, treatment with (R)-14c resulted in significant increases in urinary Na^+ normalized to creatinine (Figure 3a) and in significant decreases in urinary K^+ normalized to creatinine (Figure 3b). Consequently the Na^+/K^+ ratio at the doses of 10 and 30 mg/kg of (R)-14c at 2–4 h (Figure 3c) and 4–7 h postdose (data not shown) was significantly increased. The effect of (R)-14c was dose-dependent. Average area under the curve concentrations at the doses of 3, 10, and 30 mg/kg were respectively 1170, 9240, and 33600 ng·h/mL. These results demonstrated that (R)-14c acts as a MR antagonist.

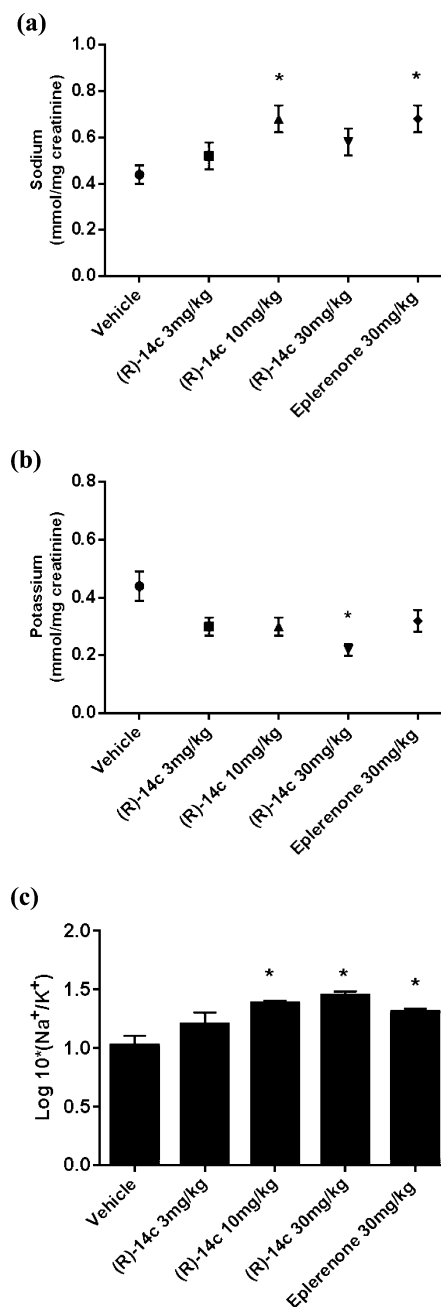


Figure 3. Effect of (R)-14c on urinary sodium (a), urinary potassium (b), and the urinary sodium to potassium ratio (Na^+/K^+ , c) in Sprague-Dawley rats. * Significantly different from vehicle ($p < 0.05$).

CONCLUSION

The search for novel potent and selective nonsteroidal MR antagonists capable of addressing the liabilities of the approved steroidal MR blockers spironolactone and eplerenone has increased over the past few years. The initial results from clinical trials with new classes of agents are starting to appear and support significant potential benefits over the steroidal agents. Our group has been engaged in the search for novel nonsteroidal MR antagonists for several years and has reported several classes of such agents. Among them is a class of potent MR antagonist based on a pyrazoline scaffold that led to the clinical candidate 2. Our efforts to follow up on this interesting compound were focused on a series of noncyclic pyrazoline analogues with two main goals in mind: improve the selectivity

versus PR to minimize the potential for sex hormone related adverse effects and improve the biopharmaceutical properties. Optimization departed from the lead **3a** characterized as a noncyclic pyrazoline analogue with good potency and selectivity. Modifications on the cyanoaryl and benzoic acid rings intended to reduce lipophilicity led not only to more polar compounds with enhanced solubility but also to analogues possessing unprecedented selectivity versus PR. Among these compounds, (*R*)-**14c** was identified as possessing excellent MR potency and higher than 500-fold selectivity versus PR in both functional and binding assays. Efforts to rationalize the potency and selectivity provided with (*R*)-**14c** using docking models did not provide a satisfactory explanation of the observed SAR, and the latter was developed primarily based on experimental observations. Using recent data from the first crystal structures of nonsteroidal MR antagonists reported by other research groups, a docking model for the binding of (*R*)-**14c** to the LBD of MR is proposed. This model not only provides a set of interactions of (*R*)-**14c** with MR consistent with the mode of binding of other MR antagonists, but it is also consistent with the SAR observed in this work. Particularly, the model depicts both acid and amide analogues able to build a similar array of interactions with MR, a feature that was not achieved by previous docking models. Pyrazoline (*R*)-**14c** was evaluated in vivo using the increase of urinary Na^+/K^+ ratio in rats as a mechanism biomarker of MR antagonism. Treatment with (*R*)-**14c** resulted in significant increases in urinary Na^+/K^+ ratio at the orally administered higher doses at 2–4 h. This effect was dose-dependent and comparable to the effect observed with eplerenone. These results demonstrated that (*R*)-**14c** acts as a MR antagonist. On the basis of the combined profile of (*R*)-**14c**, including its in vitro potency and selectivity, improved physicochemical properties, pharmacokinetic profile, and in vivo efficacy, this compound was selected for further preclinical profiling.

■ EXPERIMENTAL SECTION

General. All chemicals, reagents, and solvents were purchased from commercial sources when available and used without further purification. Proton nuclear magnetic spectroscopy (^1H NMR) was recorded with 400 and 500 MHz Varian spectrometers. Chemical shifts are expressed in parts per million downfield from tetramethylsilane. The peak shapes are denoted as follows: s, singlet; d, doublet; t, triplet; q, quartet; m, multiplet; bs, broad singlet. Mass spectrometry (MS) was performed via atmospheric pressure chemical ionization (APCI) or electron scatter (ES) ionization sources. Silica gel chromatography was performed primarily using a medium pressure Biotage or ISCO systems using columns prepackaged by various commercial vendors including Biotage and ISCO. Preparative scale separations were performed using high pressure liquid chromatography (HPLC) or supercritical fluid chromatography (SFC). Microanalyses were performed by Quantitative Technologies Inc. and were within 0.4% of the calculated values. The terms “concentrated” and “evaporated” refer to the removal of solvent at reduced pressure on a rotary evaporator with a bath temperature less than 60 °C. The abbreviations “min” and “h” stand for “minutes” and “hours”, respectively. HPLC method 1: column, Waters Symmetry C18, 3.0 mm \times 100 mm, 3.5 μm ; mobile phase A, 0.1 M ammonium acetate/acetic acid in water; mobile phase B, acetonitrile; flow rate, 0.5 mL/min; gradient, initial conditions, 0–4 min, 0–100% acetonitrile, 4–4.5 min, 100% acetonitrile, 4.5–5 min, 100–0% acetonitrile, 5–6 min, 0% acetonitrile; injection volume, 4.3 μL ; detection, UV-260 nm. HPLC Method 2: column, Waters XBridge C18, 4.6 mm \times 150 mm; 5 μm ; mobile phase A, 0.1% trifluoroacetic acid in water (v/v); mobile phase B, 0.1% trifluoroacetic acid in acetonitrile (v/v); flow rate, 1.5 mL/min; gradient, initial conditions, 0–1.5 min, 5% acetonitrile/water;

1.5–10 min, 5–100% acetonitrile/water; 10–11 min, 100% acetonitrile; 11–12.5 min, 100–5% acetonitrile/water; injection volume, 20 μL ; detection, UV-254 nm. Purity of final compounds was determined by HPLC or elemental analysis. All final compounds possess a purity of $\geq 95\%$ by HPLC or are within theoretical limits for elemental analysis (CHN), unless noted.

Synthesis of (*R*)-4-(1-(4-Cyano-3-methylphenyl)-5-cyclopentyl-4,5-dihydro-1H-pyrazol-3-yl)-2-methoxybenzoic Acid (*R*-14a**).** *Step 1: (R)-Methyl 4-(1-(4-Cyano-3-methylphenyl)-5-cyclopentyl-4,5-dihydro-1H-pyrazol-3-yl)-2-methoxybenzoate (R-13a).* *General Procedure A.* A mixture of *R*-**10**³³ (0.2 g, 0.7 mmol), 3-methoxy-4-(methoxycarbonylphenyl)boronic acid (0.11 g, 0.7 mmol), 2.0 M sodium carbonate (0.7 mL, 1.4 mmol), tetrakis-(triphenylphosphine)palladium (40 mg, 0.035 mmol), and 1,2-dimethoxyethane (3 mL) was degassed with nitrogen for 5 min and then heated at 70 °C for 16 h. The reaction was cooled to room temperature and diluted with ethyl acetate and water. The aqueous layer was extracted with ethyl acetate, and the combined organic layers were dried over magnesium sulfate, filtered, and concentrated. The residue was purified by silica gel column chromatography eluting with a gradient of ethyl acetate/heptane (0–100%) to afford *R*-**13a** as a yellow foam (0.29 mg, 100% yield): ES-MS m/z 418.2 ($M + H$).

Step 2: (R)-4-(1-(4-Cyano-3-methylphenyl)-5-cyclopentyl-4,5-dihydro-1H-pyrazol-3-yl)-2-methoxybenzoic Acid (R-14a). *General Procedure B.* To a solution of *R*-**13a** (0.367 g, 0.879 mmol) in tetrahydrofuran (4 mL) was added 2 M aqueous lithium hydroxide (2.2 mL, 4.4 mmol). The reaction was heated to 50 °C for 16 h. The mixture was cooled to room temperature, diluted with water, acidified to pH = 4 with 1N aqueous hydrochloric acid, and extracted with dichloromethane. The combined organic layers were washed with brine, dried over magnesium sulfate, filtered, and concentrated. From the concentrated mixture, *R*-**14a** was filtered and isolated as a yellow solid (0.152 g, 43%). ^1H NMR (CDCl_3 , 400 MHz): δ 9.99–10.86 (m, 1 H), 8.20 (d, J = 8.0 Hz, 1 H), 7.54 (d, J = 1.4 Hz, 1 H), 7.47 (d, J = 8.6 Hz, 1 H), 7.29 (dd, J = 8.1, 1.5 Hz, 1 H), 7.06 (d, J = 2.1 Hz, 1 H), 7.00 (dd, J = 8.5, 2.0 Hz, 1 H), 4.73 (dt, J = 11.7, 4.3 Hz, 1 H), 4.17 (s, 3 H), 3.38 (dd, J = 17.3, 11.8 Hz, 1 H), 3.06 (dd, J = 17.4, 4.3 Hz, 1 H), 2.54–2.68 (m, 1 H), 2.52 (s, 3 H), 1.73–1.89 (m, 1 H), 1.40–1.71 (m, 6 H), 0.97–1.15 (m, 1 H). ES-MS m/z 404.1 ($M + H$). HPLC purity 98%; method 2.

Synthesis of (*R*)-4-(1-(4-Cyano-3-methylphenyl)-5-cyclopentyl-4,5-dihydro-1H-pyrazol-3-yl)-2-ethoxybenzoic Acid (*R*-14b**).** *Step 1: Methyl 2-Ethoxy-4-iodobenzoate.* To a solution of methyl 4-iodosalicylate (5.0 g, 18 mmol) in DMF (55 mL) at 0 °C was added ethyl iodide (3.73 g, 23.9 mmol) slowly. The reaction was warmed to RT and stirred overnight. The reaction was diluted with dichloromethane (20 mL) and water (20 mL), and the layers were separated. The aqueous layer was extracted an additional time with dichloromethane (20 mL). The organic layers were combined, washed with brine (20 mL), dried over magnesium sulfate, filtered, and concentrated to give methyl 2-ethoxy-4-iodobenzoate as a colorless oil (5.4 g, 98%). ^1H NMR ($\text{DMSO}-d_6$, 500 MHz) δ 7.47 (s, 1 H), 7.39 (d, J = 0.7 Hz, 2 H), 4.10 (q, J = 6.8 Hz, 2 H), 3.77 (s, 3 H), 1.30 (t, J = 7.0 Hz, 3 H).

Step 2: Methyl 2-Ethoxy-4-(4,4,5,5-tetramethyl-1,3,2-dioxaborolan-2-yl)benzoate (12b). *General Procedure C.* A mixture of dichloro[1,1'-bis(diphenylphosphino)ferrocene] palladium(II) dichloromethane adduct (0.272 g, 0.33 mmol), potassium acetate (0.982 g, 9.82 mmol), and bis(pinacolato) diboron (0.913 g, 3.59 mmol) was flushed with nitrogen. Methyl 2-ethoxy-4-iodobenzoate (1.0 g, 3.27 mmol) and 1,2-dimethoxyethane (20 mL) were added. The reaction was stirred at 80 °C overnight. The reaction was cooled to room temperature and filtered through Celite. The filtrate was diluted with ethyl acetate and washed with water. The organic layer was washed with brine, dried over magnesium sulfate, and filtered. The solvent was removed to give **12b** as a brown residue that was used in the next step without further purification (0.6 g, 60%). ^1H NMR ($\text{DMSO}-d_6$, 500 MHz) δ 7.61 (d, J = 7.3 Hz, 1 H), 7.13–7.33 (m, 2 H), 4.10 (d, J = 7.1 Hz, 2 H), 3.79 (s, 3 H), 1.25–1.36 (m, 3 H), 1.17 (s, 12 H).

Step 3: (R)-Methyl 4-(1-(4-Cyano-3-methylphenyl)-5-cyclopentyl-4,5-dihydro-1H-pyrazol-3-yl)-2-ethoxybenzoate (R-13b). This compound was prepared from **R-10**³³ (300 mg, 1.04 mmol) and **12b** (0.500 g, 1.05 mmol) by the general procedure A. **R-13b** was obtained as a yellow gum (0.283 g, 63%). ¹H NMR (DMSO-*d*₆, 500 MHz) δ 7.70 (d, *J* = 8.3 Hz, 1 H), 7.56 (d, *J* = 8.8 Hz, 1 H), 7.39–7.49 (m, 2 H), 7.19 (s, 1 H), 7.11 (d, *J* = 10.0 Hz, 1 H), 4.74–5.07 (m, 1 H), 4.10–4.39 (m, 2 H), 3.80 (s, 3 H), 3.44 (dd, *J* = 17.9, 11.6 Hz, 1 H), 3.23 (dd, *J* = 18.2, 3.5 Hz, 1 H), 2.54–2.50 (m, 1 H), 2.44 (s, 3 H), 1.72–1.87 (m, 1 H), 1.45–1.66 (m, 3 H), 1.23–1.43 (m, 6 H), 0.94–1.12 (m, 1 H). ES-MS *m/z* 432.2 (*M* + *H*).

Step 4: (R)-4-(1-(4-Cyano-3-methylphenyl)-5-cyclopentyl-4,5-dihydro-1H-pyrazol-3-yl)-2-ethoxybenzoic Acid (R-14b). This compound was prepared from **R-13b** (0.28 g, 0.97 mmol) following general procedure B. **R-14b** was obtained as a yellow solid (0.243 g, 90%). ¹H NMR (DMSO-*d*₆, 500 MHz) δ 12.36–13.09 (m, 1 H), 7.68 (d, *J* = 8.5 Hz, 1 H), 7.56 (d, *J* = 8.8 Hz, 1 H), 7.38–7.45 (m, 2 H), 7.19 (s, 1 H), 7.11 (d, *J* = 8.8 Hz, 1 H), 4.60–5.06 (m, 1 H), 4.19 (quin, *J* = 7.1 Hz, 2 H), 3.36–3.54 (m, 1 H), 3.22 (dd, *J* = 17.9, 3.8 Hz, 1 H), 2.48–2.55 (m, 1 H), 2.44 (s, 3 H), 1.76 (d, *J* = 7.3 Hz, 1 H), 1.24–1.66 (m, 9 H), 0.99–1.08 (m, 1 H). ES-MS *m/z* 416.3 (*M* + *H*). HPLC purity 100%, method 1.

Synthesis of (R)-6-(1-(4-Cyano-3-methylphenyl)-5-cyclopentyl-4,5-dihydro-1H-pyrazol-3-yl)-2-methoxynicotinic Acid (R-14c). Full experimental conditions for the preparation of **(R)-14c** have been reported.³³ Pyrazoline **(R)-14c** was obtained as a crystalline solid: mp 179–181 °C. HPLC purity 99.5%. ¹H NMR (DMSO-*d*₆, 500 MHz) δ 12.94 (1H, b s), 8.11 (1H, d, *J* = 8.2 Hz), 7.66 (1H, d, *J* = 8.2 Hz), 7.56 (1H, d, *J* = 8.2 Hz), 7.22 (1H, d, *J* = 1.9 Hz), 7.10 (1H, dd, *J* = 8.6, 2.2 Hz), 4.87 (1H, dt, *J* = 11.7, 4.0 Hz), 3.94 (3H, s), 3.45 (1H, dd, *J* = 18.7, 11.9 Hz), 3.19 (1H, dd, *J* = 18.7, 4.3 Hz), 2.41 (3H, s), 1.79–1.69 (1H, m), 1.63–1.17 (7H, m), 1.08–0.95 (1H, m). MS (AP) *m/z* 405.2 (*M* + *H*)⁺. [α]_D²⁰ = +536.3° (*c* = 0.775, ACN). Anal. Calcd for C₂₃H₂₄N₄O₃: C, 68.30; H, 5.98; N, 13.85. Found C, 68.31; H, 6.05; N, 13.81.

Synthesis of (S)-6-(1-(4-Cyano-3-methylphenyl)-5-cyclopentyl-4,5-dihydro-1H-pyrazol-3-yl)-2-methoxynicotinic Acid (S-14c). **Step 1: Methyl 6-Acetyl-2-methoxynicotinate.** To a stirred solution of 6-acetyl-2-hydroxynicotinic acid⁴⁵ (2.00 g, 11 mmol) in *N,N*-dimethylformamide (30 mL) was added cesium carbonate (10.80 g, 33.1 mmol) followed by iodomethane (3.46 g, 24.3 mmol). The resulting mixture was then stirred at room temperature under nitrogen for 16 h. The mixture was filtered and washed with ethyl acetate. The filtrate was concentrated and purified by silica gel column chromatography, eluting with a gradient of ethyl acetate in heptanes (5–25%) to obtain the title compound as a solid (1.2 g, 52%). ¹H NMR (DMSO-*d*₆, 400 MHz) δ 8.28 (d, *J* = 7.79 Hz, 1 H), 7.62 (d, *J* = 7.79 Hz, 1 H), 4.02 (s, 3 H), 3.84 (s, 3 H), 2.64 (s, 3 H). ES-MS *m/z* 210.1 (*M* + *H*).

Step 2: Methyl 6-(3-Cyclopentylacryloyl)-2-methoxynicotinate (17). A solution of methyl 6-acetyl-2-methoxynicotinate (1.2 g, 5.74 mmol) and cyclopentanecarboxaldehyde (1.22 mL, 11.5 mmol) in methanol (30 mL) was stirred at 0 °C under nitrogen. Pyrrolidine (0.580 mL, 6.88 mmol) was added, and after 10 min the reaction was allowed to warm up to room temperature and stirred for 2 h. The mixture was then poured into water and extracted with ethyl acetate. The organic layer was washed with brine, dried over magnesium sulfate, concentrated, and purified by silica gel column chromatography, eluting with a gradient of ethyl acetate in heptane (0–20%) to afford **17** as a solid (0.38 g, 69%). ¹H NMR (CDCl₃, 500 MHz) δ 8.29 (d, *J* = 7.81 Hz, 1 H), 7.76 (d, *J* = 7.81 Hz, 1 H), 7.49 (dd, *J* = 0.98, 15.61 Hz, 1 H), 7.24 (dd, *J* = 8.29, 15.61 Hz, 1 H), 4.14–4.22 (m, 3 H), 3.88–4.02 (m, 3 H), 2.67–2.89 (m, 1 H), 1.86–2.00 (m, 2 H), 1.72–1.82 (m, 2 H), 1.63–1.71 (m, 2 H), 1.43–1.56 (m, 2 H). ES-MS *m/z* 290.0 (*M* + *H*).

Step 3: 6-[1-(4-Cyano-3-methylphenyl)-5-cyclopentyl-4,5-dihydro-1H-pyrazol-3-yl]-2-methoxy-nicotinic Acid (14c). To a solution of **17** (0.390 g, 1.35 mmol) and hydrazine **5**²² (0.347 g, 1.89 mmol) in ethanol (15 mL) bubbled with nitrogen was added a solution of 21% sodium ethoxide in ethanol (1.51 mL, 4.04 mmol). The mixture was heated at 80 °C for 3 h. The mixture was cooled to room temperature,

poured into a diluted hydrochloride acid solution, and extracted with ethyl acetate. The organic phase was washed with brine, dried over magnesium sulfate, and concentrated. The residue was purified by silica gel column chromatography eluting with a gradient of 0–20% methanol in dichloromethane to obtain racemic **14c** as a dark-yellow solid (0.3 g, 55%). ¹H NMR (CDCl₃, 500 MHz) δ 8.44 (d, 8.1 Hz, 1 H), 7.87 (d, *J* = 8.1 Hz, 1 H), 7.50 (d, *J* = 8.22 Hz, 1 H), 7.15 (d, *J* = 8.5 Hz, 1 H), 7.03 (dd, *J* = 8.5, 2.2 Hz, 1 H), 4.24 (s, 3 H), 4.13 (q, *J* = 7.2 Hz, 1 H), 3.44 (dd, *J* = 18.2, 12.1 Hz, 1 H), 3.27 (m, 1 H), 2.54 (s, 3 H), δ , 1.57 (m, 4 H), 1.27 (t, *J* = 7.2 Hz, 3 H), 0.89 (m, 1 H). ES-MS *m/z* 405.2 (*M* + *H*).

Step 4: (S)-6-(1-(4-Cyano-3-methylphenyl)-5-cyclopentyl-4,5-dihydro-1H-pyrazol-3-yl)-2-methoxynicotinic Acid (S-14c). This compound was obtained from the chiral separation of racemic **14c** (0.35 g, 0.865 mmol) using chiral SFC. Column, Chiralpak AD-H, 30 mm × 250 mm; mobile phase, 50% methanol/carbon dioxide; flow rate, 70 mL/min. This separation provided **S-14c** as single peak from the chiral HPLC. **S-14c** was obtained as a yellow solid (0.1 g, 29%): first eluting peak, *t*_R = 8.610 min. ¹H NMR (CDCl₃, 600 MHz) δ 9.55–11.18 (m, 1 H), 8.44 (d, *J* = 7.6 Hz, 1 H), 7.86 (d, *J* = 8.2 Hz, 1 H), 7.49 (d, *J* = 8.8 Hz, 1 H), 7.14 (d, *J* = 1.8 Hz, 1 H), 7.02 (dd, *J* = 8.5, 2.1 Hz, 1 H), 4.75 (d, *J* = 11.7 Hz, 1 H), 4.20–4.27 (s, 3 H), 3.43 (dd, *J* = 18.2, 12.3 Hz, 1 H), 3.24 (dd, *J* = 18.2, 4.1 Hz, 1 H), 2.56–2.64 (m, 1 H), 2.53 (s, 3 H), 1.25–2.10 (m, 8 H).

Synthesis of (R)-6-(1-(5-Cyano-6-methylpyridin-2-yl)-5-cyclopentyl-4,5-dihydro-1H-pyrazol-3-yl)-2-methoxynicotinic Acid (R-14d). **Step 1: 5-Cyclopentylpyrazolidin-3-one (8).** Ethyl 3-cyclopentyl acrylate³³ (450 g, 2.67 mol) was dissolved in ethanol (8.78 L) and added dropwise to a solution of hydrazine hydrate (129 mL, 133g, 2.67 mol) in ethanol (8.78 L). The solution was stirred at ambient temperature for 1 h then heated to reflux for 48 h. The reaction was then concentrated to afford a gummy yellow solid which was diluted with hexanes (1 L) and stirred for 16 h at room temperature. The resulting slurry was diluted with diethyl ether (1 L) and stirred at room temperature for 1 h. The solid was filtered off to give **8** as a beige solid (260.9 g, 63%). ¹H NMR (DMSO-*d*₆, 400 MHz) δ 8.91 (s, 1 H), 5.08 (br s, 1 H), 3.12 (br s, 1 H), 2.26 (dd, *J* = 7.48, 15.78 Hz, 1 H), 1.98 (dd, *J* = 8.31, 15.78 Hz, 1 H), 1.84 (sxt, *J* = 8.22 Hz, 1 H), 1.58–1.73 (m, 2 H), 1.38–1.56 (m, 4 H), 1.18–1.32 (m, 1 H), 1.01–1.17 (m, 1 H).

Step 2: 6-(5-Cyclopentyl-3-oxopyrazolidin-1-yl)-2-methylnicotinonitrile (7). In a microwave reaction vessel were combined **8** (11g, 72.1 mmol), 6-chloro-2-methylnicotinonitrile (**9**, 10 g, 65.4 mmol), and water (35 mL). The mixture was heated to 150 °C for 30 min in a microwave reactor. The reaction was cooled to room temperature, and the resulting solid was isolated by vacuum filtration, rinsed with water (75 mL), and dried to give the title compound as a light-brown solid (15.0 g, 87%). ¹H NMR (DMSO-*d*₆, 400 MHz) δ 10.61 (br s, 1 H), 7.89 (d, *J* = 8.59 Hz, 1 H), 6.67 (d, *J* = 8.59 Hz, 1 H), 4.74 (t, *J* = 8.01 Hz, 1 H), 2.89 (dd, *J* = 8.98, 16.41 Hz, 1 H), 2.48 (s, 3 H), 2.02–2.23 (m, 2 H), 1.71 (td, *J* = 3.81, 8.01 Hz, 1 H), 1.40–1.65 (m, 6 H), 1.15–1.33 (m, 1 H).

Step 3: 6-(3-Chloro-5-cyclopentyl-4,5-dihydro-1H-pyrazol-1-yl)-2-methylnicotinonitrile (11). A mixture of **7** (140 g, 518 mmol) in acetonitrile (6 L) was treated with phosphoryl chloride (53 mL, 570 mmol) and heated to 80 °C for 2 h. The reaction was stirred overnight at room temperature. The reaction was concentrated to dark-brown solid that were dissolved in dichloromethane and washed with saturated sodium bicarbonate, brine, dried over sodium sulfate, and filtered. The organic layer was concentrated. The residue was purified by silica gel column chromatography eluting with a gradient of 5–40% ethyl acetate/heptane to provide **11** (131.4 g, 79%) as a rose-colored solid. ¹H NMR (DMSO-*d*₆, 400 MHz) δ 7.79 (d, *J* = 8.59 Hz, 1 H), 6.91 (d, *J* = 8.59 Hz, 1 H), 4.90 (td, *J* = 4.79, 11.52 Hz, 1 H), 3.44 (dd, *J* = 11.72, 18.36 Hz, 1 H), 2.93 (dd, *J* = 4.69, 18.36 Hz, 1 H), 2.58–2.76 (m, 1 H), 2.47 (s, 3 H), 1.35–1.76 (m, 6 H), 1.05–1.29 (m, 2 H). (ES-MS) *m/z* 289.1 (*M* + *H*).

Step 4: (R)-6-(3-Chloro-5-cyclopentyl-4,5-dihydro-1H-pyrazol-1-yl)-2-methylnicotinonitrile (R-11). This compound was obtained from **11** using chiral SFC (column: Chiralpak AD-H, 30 mm × 250 mm;

mobile phase, 10% 2-propanol/carbon dioxide; flow rate, 70 mL/min). First eluting peak: chiral HPLC t_R = 1.76 (Chiralpak AD-H, 20% 2-propanol/carbon dioxide). ^1H NMR (DMSO- d_6 , 400 MHz) δ 7.79 (d, J = 8.79 Hz, 1 H), 6.91 (d, J = 8.79 Hz, 1 H), 4.90 (td, J = 4.91, 11.48 Hz, 1 H), 3.45 (dd, J = 11.53, 18.37 Hz, 1 H), 2.93 (dd, J = 4.79, 18.47 Hz, 1 H), 2.60–2.73 (m, 1 H), 1.37–1.70 (m, 6 H), 1.03–1.28 (m, 2 H). (ES-MS) m/z 289.1 (M + H).

Step 5: (R)-Methyl 6-(1-(5-Cyano-6-methylpyridin-2-yl)-5-cyclopentyl-4,5-dihydro-1H-pyrazol-3-yl)-2-methoxynicotinate (R-13d). This compound was prepared following general procedure A from **R-11** (90 mg, 0.31 mmol) and methyl 2-methoxy-6-(4,4,5,5-tetramethyl-1,3,2-dioxaborolan-2-yl)-nicotinate³³ (**12c**, 100 mg, 0.34 mmol). Purification by silica gel column chromatography eluting with a gradient of ethyl acetate/heptane (0–100%) afforded **R-13d** as a yellow solid (50 mg, 38% yield). ^1H NMR (DMSO- d_6 , 500 MHz) δ 8.15–8.34 (m, 1 H), 7.87–7.99 (m, 1 H), 7.64–7.84 (m, 1 H), 7.18–7.42 (m, 1 H), 4.70–5.19 (m, 1 H), 4.00 (s, 3 H), 3.82 (s, 3 H), 3.47–3.60 (m, 1 H), 3.16–3.27 (m, 1 H), 2.77–2.92 (m, 1 H), 2.54 (s, 3 H), 1.68–1.76 (m, 1 H), 1.57–1.65 (m, 1 H), 1.47–1.56 (m, 2 H), 1.36–1.46 (m, 2 H), 1.28–1.35 (m, 1 H), 1.05–1.14 (m, 1 H). (ES-MS) m/z 420.3 (M + H).

Step 6: (R)-6-(1-(5-Cyano-6-methylpyridin-2-yl)-5-cyclopentyl-4,5-dihydro-1H-pyrazol-3-yl)-2-methoxynicotinic Acid (R-14d). This compound was prepared following general procedure B from **R-13d** (0.30 g, 0.715 mmol). **R-14d** was isolated as a yellow solid (0.202 g, 70%). ^1H NMR (DMSO- d_6 , 500 MHz) δ 12.84–13.14 (m, 1 H), 8.17 (d, J = 7.81 Hz, 1 H), 7.90 (d, J = 8.78 Hz, 1 H), 7.72 (d, J = 7.81 Hz, 1 H), 7.27 (d, J = 8.78 Hz, 1 H), 5.01 (td, J = 4.57, 11.59 Hz, 1 H), 3.98 (s, 3 H), 3.52 (dd, J = 11.71, 18.54 Hz, 1 H), 3.15–3.25 (m, 1 H), 2.78–2.91 (m, 1 H), 2.54 (s, 3 H), 1.67–1.74 (m, 1 H), 1.37–1.65 (m, 6 H), 1.26–1.34 (m, 1 H). ES-MS m/z 406.2 (M + H). HPLC purity 96%, method 1.

Synthesis of (R)-4-(1-(5-Cyano-6-methylpyridin-2-yl)-5-cyclopentyl-4,5-dihydro-1H-pyrazol-3-yl)-2-methoxybenzoic Acid (R-14e). To a solution of **R-11** (503 mg, 1.74 mmol) and 4-boron-2-methoxybenzoic acid (355 mg, 1.81 mmol) in 1,2-dimethoxyethane (15 mL) was added 2 M sodium carbonate (2.62 mL) followed by tetrakis(triphenylphosphine) palladium (98 mg, 0.085 mmol). The reaction mixture was refluxed for 15 h under nitrogen. Preparative HPLC (reverse phase, acetonitrile/water) provided **R-14e** as a solid (248 mg, 35%). ^1H NMR (DMSO- d_6 , 400 MHz) δ 7.83 (d, J = 8.78 Hz, 1 H), 7.69 (d, J = 8.05 Hz, 1 H), 7.46 (s, 1 H), 7.41 (d, J = 8.05 Hz, 1 H), 7.25 (d, J = 8.78 Hz, 1 H), 4.86–5.23 (m, 1 H), 3.89 (s, 3 H), 3.46 (dd, J = 11.35, 17.93 Hz, 1 H), 3.14–3.23 (m, 1 H), 2.78 (m, 1 H), 2.53 (s, 3 H), 1.28–1.84 (m, 7 H), 1.09 (m, 1 H). ES-MS m/z 405.2 (M + H). HPLC purity 93%, method 2.

Synthesis of (R)-4-(1-(5-Cyano-6-methylpyridin-2-yl)-5-cyclopentyl-4,5-dihydro-1H-pyrazol-3-yl)benzoic Acid (R-14f). A mixture of **R-11** (200 mg, 0.69 mmol), 4-boronobenzoic acid (115 mg, 0.69 mmol), and palladium tetrakis triphenylphosphine (40 mg, 0.035 mmol) were suspended in acetonitrile (7 mL) and 0.4 M aqueous sodium carbonate (7 mL). The mixture was heated to 90 °C for 4 h. The reaction mixture was cooled, and the reaction was concentrated to remove the acetonitrile. To the residue was added ethyl acetate, and the layers were separated. The aqueous layer was washed with ethyl acetate three times. The aqueous layer was acidified with concentrated hydrochloric acid, and a brownish-green precipitate formed. This precipitate was collected by filtration and dried to provide **R-14f** as a green solid (61 mg, 22%). ^1H NMR (CH₃OH- d_4 , 400 MHz) δ 8.08 (d, J = 8.60 Hz, 2 H), 7.95 (d, J = 8.60 Hz, 2 H), 7.80 (d, J = 8.99 Hz, 1 H), 7.30 (d, J = 8.99 Hz, 1 H), 4.97–5.16 (m, 1 H), 3.51 (dd, J = 11.14, 17.98 Hz, 1 H), 3.24 (dd, J = 4.20, 18.08 Hz, 1 H), 2.77–2.90 (m, 1 H), 2.62 (s, 3 H), 1.31–1.87 (m, 7 H), 0.91–1.27 (m, 1 H). ES-MS m/z 375.1 (M + H). HPLC purity 96%, method 2.

Synthesis of (R)-6-(1-(4-Cyano-3-methylphenyl)-5-cyclopentyl-4,5-dihydro-1H-pyrazol-3-yl)-2-ethoxynicotinic Acid (R-14g). **Step 1: Ethyl 2,6-Dichloronicotinate.** To a solution of 2,6-dichloronicotinic acid (10 g, 52.08 mmol) in ethanol (50 mL) was added concentrated sulfuric acid (1.0 mL), and the mixture was heated

to reflux for 16 h. The reaction was concentrated. The solid residue was diluted with ethyl acetate (50 mL) and washed with water (50 mL), 1 M aqueous sodium carbonate (50 mL), and saturated aqueous sodium chloride. The organic layer was dried over magnesium sulfate, filtered, and concentrated to give the desired compound as a light-orange solid (7.38 g, 65%). ^1H NMR (DMSO- d_6 , 500 MHz) δ 8.31 (d, J = 8.05 Hz, 1 H), 7.72 (d, J = 8.05 Hz, 1 H), 4.35 (q, J = 7.24 Hz, 2 H), 1.32 (t, J = 7.07 Hz, 3 H).

Step 2: Ethyl 6-Chloro-2-ethoxynicotinate. To a solution of ethyl 2,6-dichloronicotinate (5.0 g, 22.72 mmol) in dichloromethane (25 mL) at 0 °C was added sodium ethoxide (2.12 g, 29.5 mmol) slowly. The reaction was stirred at 0 °C for 3 h and then warmed to ambient temperature over 16 h. The reaction was diluted with dichloromethane (20 mL) and water (20 mL), and the layers were separated. The aqueous layer was extracted an additional time with dichloromethane (20 mL). The organic layers were combined, washed with brine (20 mL), dried over magnesium sulfate, filtered, and concentrated to give ethyl 6-chloro-2-ethoxynicotinate as a light-yellow solid (4.38 g, 84%). ^1H NMR (DMSO- d_6 , 400 MHz) δ 8.11 (d, J = 8.00 Hz, 1 H), 7.14 (d, J = 8.00 Hz, 1 H), 4.33 (q, J = 7.03 Hz, 2 H), 4.23 (q, J = 7.03 Hz, 2 H), 1.23–1.33 (m, 6 H).

Step 3: Ethyl 2-Ethoxy-6-(4,4,5,5-tetramethyl-1,3,2-dioxaborolan-2-yl)nicotinate (12g). A mixture of dichloro[1,1'-bis-(diphenylphosphino)ferrocene]palladium(II) dichloromethane adduct (0.124 g, 0.166 mmol), potassium acetate (0.497 g, 4.96 mmol), and bis(pinacolato) diboron (0.462 g, 1.82 mmol) was flushed with nitrogen. Ethyl 6-chloro-2-ethoxynicotinate (0.400 g, 1.74 mmol) and 1,2-dimethoxyethane (5 mL) were added. The reaction was stirred at 80 °C overnight. The reaction was cooled to room temperature and filtered through Celite. The filtrate was diluted with ethyl acetate and washed with water. The organic layer was washed with brine, dried over magnesium sulfate, and filtered. The solvent was removed to give **12g** as a brown residue that was used for the next step without further purification (0.559 g). ^1H NMR (DMSO- d_6 , 500 MHz) δ 8.03 (J = 7.32 Hz, 1 H), 7.42 (J = 7.32 Hz, 1 H), 4.40 (q, J = 7.07 Hz, 2 H), 4.20 (q, J = 7.07 Hz, 2 H), 1.26–1.38 (m, 12 H), 1.07–1.20 (m, 6 H).

Step 4: (R)-Ethyl 6-(1-(4-Cyano-3-methylphenyl)-5-cyclopentyl-4,5-dihydro-1H-pyrazol-3-yl)-2-ethoxynicotinate (R-13g). This compound was prepared from **R-10**³³ (375 mg, 1.30 mmol) and **12g** (0.500 g, 1.56 mmol) following general procedure A. **R-13g** was obtained as a yellow gum (0.507 g, 88%). ^1H NMR (DMSO- d_6 , 500 MHz) δ 8.13 (d, J = 7.81 Hz, 1 H), 7.68 (d, J = 8.05 Hz, 1 H), 7.60 (d, J = 8.78 Hz, 1 H), 7.24 (s, 1 H), 7.14 (dd, J = 2.07, 8.66 Hz, 1 H), 4.89 (td, J = 3.96, 11.83 Hz, 1 H), 4.39–4.58 (m, 2 H), 4.27 (q, J = 7.07 Hz, 2 H), 3.46 (dd, J = 11.83, 11.8 Hz, 1 H), 3.19 (dd, J = 4.03, 18.42 Hz, 1 H), 2.49–2.63 (m, 1 H), 2.44 (s, 3 H), 1.77 (dd, J = 4.03, 7.68 Hz, 1 H), 1.58 (d, J = 6.83 Hz, 1 H), 1.48–1.54 (m, 2 H), 1.33–1.45 (m, 4 H), 1.20–1.32 (m, 5 H), 0.99–1.13 (m, 1 H). ES-MS m/z 447.2 (M + H).

Step 5: (R)-6-(1-(4-Cyano-3-methylphenyl)-5-cyclopentyl-4,5-dihydro-1H-pyrazol-3-yl)-2-ethoxynicotinic Acid (R-14g). This compound was prepared from **R-13g** (0.5 g, 1.12 mmol) following general procedure B. **R-14g** was obtained as a yellow solid (0.46 g, 98%). ^1H NMR (DMSO- d_6 , 500 MHz) δ 12.62–13.08 (m, 1 H), 8.12 (d, J = 7.81 Hz, 1 H), 7.67 (d, J = 7.81 Hz, 1 H), 7.59 (d, J = 8.54 Hz, 1 H), 7.25 (d, J = 1.71 Hz, 1 H), 7.13 (dd, J = 2.20, 8.78 Hz, 1 H), 4.89 (td, J = 4.06, 11.65 Hz, 1 H), 4.30–4.60 (m, 2 H), 3.41–3.53 (m, 1 H), 3.20 (dd, J = 4.15, 18.30 Hz, 1 H), 2.53 (d, J = 3.90 Hz, 1 H), 2.44 (s, 3 H), 1.77 (dd, J = 3.42, 7.07 Hz, 1 H), 1.59 (d, J = 8.54 Hz, 2 H), 1.47–1.55 (m, 2 H), 1.20–1.44 (m, 5 H), 1.04 (dd, J = 9.64, 12.56 Hz, 1 H). ES-MS m/z 419.2 (M + H). HPLC purity 100%, method 1.

Synthesis of (R)-6-[1-(3-Chloro-4-cyano-phenyl)-5-cyclopentyl-4,5-dihydro-1H-pyrazol-3-yl]-2-methoxy-nicotinic Acid (R-19). **Step 1: 6-[1-(3-Chloro-4-cyano-phenyl)-5-cyclopentyl-4,5-dihydro-1H-pyrazol-3-yl]-2-methoxy-nicotinic Acid (19).** To a solution of **17** (0.258 g, 0.892 mmol) and 2-chloro-4-hydrazino-benzonitrile²² (0.255 g, 1.25 mmol) in ethanol (8.9 mL) bubbled with argon was added a solution of 21% sodium ethoxide in ethanol (1 mL, 2.68 mmol). The mixture was heated to 80 °C for 2 h under nitrogen. After this time, it was cooled, poured into diluted HCl solution, and

extracted with ethyl acetate. The combined ethyl acetate phase was washed with brine, dried over sodium sulfate, and concentrated. The residue was purified by chromatography (reverse phase, acetonitrile/water) to obtain **19** as a solid (0.160 g, 42%). ¹H NMR (DMSO-*d*₆, 400 MHz) δ 8.15 (d, *J* = 8.05 Hz, 1 H), 7.75 (d, *J* = 7.69 Hz, 1 H), 7.73 (d, *J* = 6.59 Hz, 1 H), 7.45 (d, *J* = 2.20 Hz, 1 H), 7.24 (dd, *J* = 8.97, 2.01 Hz, 1 H), 4.94 (td, *J* = 7.59, 3.48 Hz, 1 H), 3.98 (s, 3 H), 3.51 (dd, *J* = 18.48, 11.53 Hz, 1 H), 3.24 (dd, *J* = 18.48, 11.53 Hz, 1 H), 2.43–2.48 (m, 1 H), 1.73–1.82 (m, 1 H), 1.21–1.64 (m, 6 H), 0.99–1.10 (m, 1 H). ES-MS *m/z* 439.0 (M + H).

Step 2: (R)-6-[1-(3-Chloro-4-cyano-phenyl)-5-cyclopentyl-4,5-dihydro-1H-pyrazol-3-yl]-2-methoxy-nicotinic Acid (R-19). Separation of the enantiomers of **19** (0.160 g, 0.337 mmol) using chiral HPLC (SFC conditions): Chiralpak AD-H, 30 mm × 250 mm; mobile phase, 50% methanol/carbon dioxide; flow rate, 70 mL/min. This separation provided **R-19** as a single peak from the chiral HPLC. **R-19** was obtained as yellow solid (0.063 g, 39%): first eluting peak *t*_R = 7.395 min. ¹H NMR (DMSO-*d*₆, 500 MHz) δ 12.59–13.22 (m, 1 H), 8.15 (d, *J* = 7.8 Hz, 1 H), 7.75 (dd, *J* = 10.7, 8.3 Hz, 2 H), 7.47 (d, *J* = 2.2 Hz, 1 H), 7.25 (dd, *J* = 8.9, 2.1 Hz, 1 H), 4.95 (dt, *J* = 11.5, 3.9 Hz, 1 H), 3.98 (s, 3 H), 3.46–3.58 (m, 1 H), 3.25 (dd, *J* = 18.4, 3.8 Hz, 1 H), 2.43–2.48 (m, 1 H), 1.72–1.86 (m, 1 H), 1.19–1.67 (m, 6 H), 0.98–1.07 (m, 1 H). ES-MS *m/z* 425.0 (M + H).

Synthesis of (R)-6-[1-(4-Cyano-3-methylphenyl)-5-cyclopentyl-4,5-dihydro-1H-pyrazol-3-yl]-2-methoxynicotinamide (R-16a). **Step 1: 6-Bromo-2-methoxy-nicotinic Acid.** A solution of 2,2,6,6-tetramethylpiperidine (0.766 g, 5.32 mmol) in tetrahydrofuran (5 mL) was cooled to –78 °C under nitrogen, then 2.5 M *n*-butyllithium in hexanes (2.34 mL, 0.375 g, 5.85 mmol) was added and the mixture was stirred at –78 °C for 30 min. To the reaction mixture was added a solution of 2-bromo-6-methoxypyridine (1.00 g, 5.32 mmol) in tetrahydrofuran (5 mL) dropwise. The reaction was stirred at –78 °C for 1 h. After this time, an excess of dry ice was added to the reaction mixture and the reaction was allowed to warm to room temperature for 3 h. To the mixture was added water and ethyl acetate, and the layers were separated. The aqueous layer was acidified to pH 4. The aqueous layer was extracted 3 times with ethyl acetate. The combined organic layers were washed with brine, dried over magnesium sulfate, filtered, and concentrated to give an off-white solid (0.530 g, 43%). ¹H NMR (DMSO-*d*₆, 500 MHz) δ 12.87–13.40 (m, 1 H), 8.03 (d, *J* = 7.8 Hz, 1 H), 7.33 (d, *J* = 7.8 Hz, 1 H), 3.90 (s, 3 H).

Step 2: 6-Bromo-2-methoxy-nicotinic Acid Methyl Ester. To potassium carbonate (1.34 g, 9.48 mmol) in *N,N*-dimethylformamide (10 mL) was added 6-bromo-2-methoxy-nicotinic acid (1.10 g, 4.74 mmol) and methyl iodide (0.895 g, 6.31 mmol). The reaction was stirred for 16 h at room temperature. The reaction mixture was diluted with water and ethyl acetate, and the layers were separated. The aqueous layer was washed with ethyl acetate 2 times. The combined organic layers were washed with brine and dried over magnesium sulfate, filtered, and concentrated. The filtrate was concentrated and purified by silica gel column chromatography, eluting with a gradient of 5–10% ethyl acetate/heptane to obtain the title compound as a colorless oil (0.459 g, 40%). ¹H NMR (DMSO-*d*₆, 500 MHz) δ 8.06 (d, *J* = 7.81 Hz, 1 H), 7.36 (d, *J* = 7.81 Hz, 1 H), 3.93 (s, 3 H), 3.81 (s, 3 H).

Step 3: 6-Bromo-2-methoxy-nicotinamide. 6-Bromo-2-methoxy-nicotinic acid methyl ester (0.45 g, 183 mmol) and ammonium hydroxide (5 mL) were combined in a sealed tube and heated to 70 °C for 3 h. The reaction was cooled to room temperature, filtered, and rinsed with water to obtain the title compound as a white solid (0.278 g, 66%). ¹H NMR (DMSO-*d*₆, 500 MHz) δ 8.05 (d, *J* = 7.81 Hz, 1 H), 7.59–7.89 (m, 2 H), 7.35 (d, *J* = 7.81 Hz, 1H), 3.96 (s, 3 H).

Step 4: 2-Methoxy-6-(4,4,5,5-tetramethyl-[1,3,2]dioxaborolan-2-yl)-nicotinamide (15a). This compound was prepared from 6-bromo-2-methoxy-nicotinamide (0.270 g, 1.17 mmol) by the general procedure C. The title compound was isolated as a brown liquid (0.325 g, 100%). ¹H NMR (DMSO-*d*₆, 500 MHz) δ 8.11 (d, *J* = 7.3 Hz, 1 H), 7.63 (d, *J* = 7.3 Hz, 1 H), 7.51 (br s Two H), 3.98 (s, 3 H), 1.16 (s, 12 H).

Step 5: (R)-6-[1-(4-Cyano-3-methylphenyl)-5-cyclopentyl-4,5-dihydro-1H-pyrazol-3-yl]-2-methoxynicotinamide (R-16a). The title compound was prepared from **R-10** (0.174 g, 0.605 mmol) and 2-methoxy-6-(4,4,5,5-tetramethyl-[1,3,2]dioxaborolan-2-yl)-nicotinamide (0.202 g, 0.726 mmol) following general procedure A. **R-16a** was obtained as a yellow solid (0.035 g, 14%). ¹H NMR (DMSO-*d*₆, 400 MHz) δ 8.19 (d, *J* = 7.81 Hz, 1 H), 7.70 (d, *J* = 7.81 Hz, 1 H), 7.67 (d, *J* = 3.12 Hz, 2 H), 7.56 (d, *J* = 8.78 Hz, 1 H), 7.21 (d, *J* = 1.95 Hz, 1 H), 7.10 (dd, *J* = 2.24, 8.69 Hz, 1 H), 4.86 (d, *J* = 11.71 Hz, 1 H), 4.01 (s, 3 H), 3.38–3.54 (dd, *J* = 4.00, 18.45 Hz, 1 H), 3.19 (dd, *J* = 4.00, 18.45 Hz, 1 H), 2.48–2.56 (m, 1 H), 2.41 (s, 3 H), 1.66–1.86 (m, 1 H), 1.48 (d, *J* = 8.59 Hz, 3 H), 1.18–1.40 (m, 3 H), 0.86–1.11 (m, 1 H). ES-MS *m/z* 404.3 (M + H). HPLC purity 100%, method 1.

Synthesis of (R)-6-[1-(4-Cyano-3-methylphenyl)-5-cyclopentyl-4,5-dihydro-1H-pyrazol-3-yl]-2-methoxy-N-methylnicotinamide (R-16b). **General Procedure D.** To a solution of carboxylic acid **R-14c** (0.10 g, 0.247 mmol) in DMF (0.5 mL) was added CDI (0.061 g, 0.370 mmol). The mixture was stirred for 20 min, and then a 2 M solution of methylamine in THF (1.24 mL, 2.47 mmol) was added. The reaction stirred overnight at RT. The reaction was diluted with ethyl acetate and water, and the layers were separated. The aqueous layer was washed an additional ethyl acetate twice. The combined organic layers were washed with brine and dried over magnesium sulfate, filtered, and concentrated to provide pure **R-16b** as a yellow solid (0.094 g, 92%). ¹H NMR (DMSO-*d*₆, 500 MHz) δ 8.27–8.22 (m, 1 H), 8.20 (d, *J* = 7.8 Hz, 1 H), 7.73 (d, *J* = 7.8 Hz, 1 H), 7.59 (d, *J* = 8.8 Hz, 1 H), 7.24 (d, *J* = 1.7 Hz, 1 H), 7.16–7.06 (m, 1 H), 4.95–4.82 (m, 1 H), 4.04 (s, 3 H), 3.57–3.43 (m, 1 H), 3.29–3.19 (m, 1 H), 2.83 (d, *J* = 4.6 Hz, 3 H), 2.51 (m, 1 H), 2.44 (s, 3 H), 1.83–1.72 (m, 1 H), 1.65–1.56 (m, 1 H), 1.55–1.46 (m, 2 H), 1.44–1.35 (m, 1 H), 1.34–1.22 (m, 2 H), 1.13–1.02 (m, 1 H). ES-MS *m/z* 418.2 (M + H). HPLC purity 100%, method 1.

Synthesis of (R)-6-[1-(4-Cyano-3-methylphenyl)-5-cyclopentyl-4,5-dihydro-1H-pyrazol-3-yl]-2-methoxy-N,N-dimethylnicotinamide (R-16c). This compound was prepared from carboxylic acid **R-14c** (0.048 g, 0.12 mmol) and a 2 M solution of dimethylamine in tetrahydrofuran (0.595 mL, 1.19 mmol) following general procedure D. **R-16c** was obtained as a yellow solid (0.036 g, 71%). ¹H NMR (DMSO-*d*₆, 500 MHz) δ 7.66–7.76 (m, 2 H), 7.58 (d, *J* = 8.5 Hz, 1 H), 7.23 (d, *J* = 2.0 Hz, 1H), 7.12 (dd, *J* = 8.7, 2.1 Hz, 1 H), 4.67–4.95 (m, 1 H), 3.96 (s, 3 H), 3.48 (dd, *J* = 18.4, 11.6 Hz, 1 H), 3.22 (dd, *J* = 18.11.6 Hz, 1 H), 2.98 (s, 3 H), 2.81 (s, 3 H), 2.50–2.60 (m, 1 H), 2.44 (s, 3 H), 1.77 (d, *J* = 8.1 Hz, 1 H), 1.47–1.65 (m, 3 H), 1.22–1.44 (m, 3 H), 1.08 (d, *J* = 9.3 Hz, 1 H). ES-MS *m/z* 432.3 (M + H). HPLC purity 100%, method 1.

Synthesis of (R)-6-[1-(5-Cyano-6-methylpyridin-2-yl)-5-cyclopentyl-4,5-dihydro-1H-pyrazol-3-yl]-2-methoxynicotinamide (R-16d). This compound was prepared from chloropyrazoline **R-11** (0.175 g, 0.606 mmol) and boronate **15a** (0.202 g, 0.727 mmol) following general procedure A. Purification by silica gel column chromatography eluting with a gradient of methanol in dichloromethane (0–9%) with ammonium hydroxide gave amide **R-16d** as a yellow solid (0.034 g, 14%). ¹H NMR (DMSO-*d*₆, 500 MHz) δ 8.24 (d, *J* = 7.8 Hz, 1 H), 7.90 (d, *J* = 8.8 Hz, 1 H), 7.76 (d, *J* = 7.8 Hz, 1 H), 7.73 (d, *J* = 8.8 Hz, 2 H), 7.27 (d, *J* = 8.8 Hz, 1 H), 5.01 (dt, *J* = 11.6, 4.6 Hz, 1 H), 4.04 (s, 3 H), 3.52 (dd, *J* = 18.7, 11.6 Hz, 1 H), 3.20 (dd, *J* = 18.5, 4.6 Hz, 1 H), 2.83 (d, *J* = 4.6 Hz, 1 H), 2.54 (s, 3 H), 1.71 (dd, *J* = 12.0, 4.1 Hz, 1 H), 1.58–1.65 (m, 1 H), 1.48–1.58 (m, 2 H), 1.28–1.47 (m, 3 H), 1.11–1.18 (m, 1 H). ES-MS *m/z* 405.3 (M + H). HPLC purity 97%, method 1.

Synthesis of (R)-6-[1-(5-Cyano-6-methylpyridin-2-yl)-5-cyclopentyl-4,5-dihydro-1H-pyrazol-3-yl]-2-methoxy-N-methylnicotinamide (R-16e). This compound was prepared from carboxylic acid **R-14d** (0.10 g, 0.247 mmol) and a 2 M solution of methylamine in tetrahydrofuran (1.23 mL, 2.47 mmol) following general procedure D. **R-16e** was obtained as a yellow solid (0.097 g, 62%). ¹H NMR (DMSO-*d*₆, 500 MHz) δ 8.24–8.29 (m, 1 H), 8.21 (d, *J* = 7.8 Hz, 1 H), 7.89 (d, *J* = 8.8 Hz, 1 H), 7.75 (d, *J* = 7.8 Hz, 1 H), 7.26 (d, *J* = 8.8 Hz, 1 H), 4.85–5.09 (m, 1 H), 4.04 (s, 3 H), 3.44–3.59 (m, 1 H), 3.17–3.33 (m, 1 H), 2.83 (m, 4 H), 2.54 (s, 3 H), 1.66–1.82 (m, 1 H), 1.59–1.66 (m, 1 H), 1.49–1.58 (m, 2 H), 1.26–1.47 (m, 3 H), 1.06–

1.15 (m, 1 H). ES-MS M/Z 419.2 ($M + H$). HPLC purity 95%, method 1.

Synthesis of (R)-6-(1-(5-Cyano-6-methylpyridin-2-yl)-5-cyclopentyl-4,5-dihydro-1H-pyrazol-3-yl)-2-methoxy-N,N-dimethylnicotinamide (R-16f). This compound was prepared from carboxylic acid **R-14d** (0.10 g, 0.247 mmol) and a 2 M solution of dimethylamine in tetrahydrofuran (1.24 mL, 2.47 mmol) following general procedure D. **R-16f** was obtained as a white solid (0.081 g, 76%). 1H NMR (DMSO- d_6 , 500 MHz) δ 7.88 (d, $J = 9.0$ Hz, 1 H), 7.62–7.77 (m, 2 H), 7.25 (d, $J = 9.0$ Hz, 1 H), 4.99 (dt, $J = 11.4, 4.7$ Hz, 1 H), 3.97 (s, 3 H), 3.52 (dd, $J = 18.7, 11.6$ Hz, 1 H), 3.20 (dd, $J = 18.5, 4.6$ Hz, 1 H), 2.99 (s, 3 H), 2.76–2.87 (m, 4 H), 2.54 (s, 3 H), 1.66–1.76 (m, 1 H), 1.59–1.65 (m, 1 H), 1.49–1.58 (m, 2 H), 1.28–1.47 (m, 3 H), 1.07–1.16 (m, 1 H). ES-MS m/z 433.3 ($M + H$). HPLC purity 100%, method 1.

Synthesis of 6-((R)-1-(5-Cyano-6-methylpyridin-2-yl)-5-isopropyl-4,5-dihydro-1H-pyrazol-3-yl)-2-methoxynicotinic Acid (R-25). **Step 1:** 6-Hydrazinyl-2-methylnicotinonitrile (**21**). To a suspension of **8** (1.04 g, 6.84 mmol) in ethanol (6.8 mL) was added hydrazine monohydrate (0.51 mL, 10.3 mmol). The mixture was heated at 80 °C overnight with the formation of solid as the reaction progressed. The reaction mixture was cooled in an ice-bath. The solid was separated by filtration, washed with cool ethanol, and dried under vacuum. **21** was obtained as yellow solid (1.01 g, 100%). 1H NMR (DMSO- d_6 , 400 MHz) δ 8.49 (br s, 1 H), 7.66 (d, $J = 8.9$ Hz, 1 H), 6.61 (br s, 1 H), 4.43 (br s, 2 H), 2.41 (s, 3 H).

Step 2: 6-(5-Isopropyl-3-oxopyrazolidin-1-yl)-2-methylnicotinonitrile (**22**). To a solution of methyl 4-methylpent-2-enoate (3 g, 23.4 mmol) and hydrazine **21** (4.3 g, 29 mmol) in ethanol (50 mL) sparged with nitrogen was added potassium *t*-butoxide (8.29 g, 70.2 mmol). The mixture was heated at 80 °C overnight. The mixture was cooled to room temperature, poured into a diluted hydrochloric acid solution, and extracted with ethyl acetate. The organic phase was washed with brine, dried over magnesium sulfate, and concentrated. The residue was purified by silica gel column chromatography eluting with a gradient of ethyl acetate in heptanes (0–100%) to obtain **22** as a solid (1.58 g, 28%). 1H NMR (CDCl₃, 400 MHz) δ 7.64 (d, $J = 8.8$ Hz, 1 H), 6.52 (d, $J = 8.6$ Hz, 1 H), 4.42 (ddd, $J = 9.7, 6.2, 2.0$ Hz, 1 H), 2.89 (dd, $J = 17.3, 9.7$ Hz, 1 H), 2.58–2.64 (m, 4 H), 2.43 (dd, $J = 17.3, 2.0$ Hz, 1 H), 1.98–2.15 (m, 1 H), 1.02 (dd, $J = 6.8, 1.4$ Hz, 6H). ES-MS m/z 245.2 ($M + H$).

Step 3: 6-(3-Chloro-5-isopropyl-4,5-dihydro-1H-pyrazol-1-yl)-2-methylnicotinonitrile (**23**). A mixture of **22** (0.75 g, 3.07 mmol) in acetonitrile (10 mL) was treated with phosphoryl chloride (0.87 mL, 9.21 mmol) and heated to 80 °C for 3 h. The reaction was stirred overnight at room temperature. The reaction was concentrated to dark-brown solid that were dissolved in dichloromethane and washed with saturated sodium bicarbonate, brine, dried over sodium sulfate, and filtered. The organic layer was concentrated. The residue was triturated by ether (15 mL). The resulting precipitate was collected by filtration and rinsed by ether and dried to yield **23** as a light-yellow solid (0.368 g, 46%). 1H NMR (CDCl₃, 400 MHz) δ 7.56 (d, $J = 9.0$ Hz, 1 H), 7.02 (d, $J = 9.0$ Hz, 1 H), 4.78 (ddd, $J = 11.9, 5.5, 3.9$ Hz, 1 H), 3.15 (dd, $J = 18.2, 11.8$ Hz, 1 H), 2.87 (dd, $J = 18.2, 5.6$ Hz, 1 H), 2.71 (td, $J = 7.0, 3.8$ Hz, 1 H), 2.56 (s, 3 H), 0.91 (d, $J = 7.0$ Hz, 3 H), 0.75 (d, $J = 7.0$ Hz, 3 H). ES-MS m/z 263.1 ($M + H$).

Step 4: Methyl 6-(1-(5-Cyano-6-methylpyridin-2-yl)-5-isopropyl-4,5-dihydro-1H-pyrazol-3-yl)-2-methoxynicotinate (**24**). This compound was prepared from **23** (0.15 g, 0.57 mmol) and boronate **12c** (0.167 g, 0.57 mmol) following general procedure A. Ester **24** was obtained as a solid (0.225 g, 45%). 1H NMR (CDCl₃, 400 MHz) δ 8.18 (d, $J = 7.8$ Hz, 1 H), 7.68 (d, $J = 8.0$ Hz, 1 H), 7.62 (d, $J = 8.8$ Hz, 1 H), 7.29 (d, $J = 8.8$ Hz, 1 H), 4.74–4.95 (m, 1 H), 4.08 (s, 3 H), 3.83–3.98 (m, 3 H), 3.16–3.42 (m, 2 H), 2.72–2.95 (m, 1 H), 2.62 (s, 3 H), 0.99 (d, $J = 7.0$ Hz, 3 H), 0.68 (d, $J = 7.0$ Hz, 3 H). ES-MS m/z 394.1 ($M + H$).

Step 5: 6-(1-(5-Cyano-6-methylpyridin-2-yl)-5-isopropyl-4,5-dihydro-1H-pyrazol-3-yl)-2-methoxynicotinic acid (**25**). This compound was prepared from **24** (0.1 g, 0.25 mmol) following general procedure B. Racemic acid **25** was obtained as a bright solid (0.082 g, 85%). 1H NMR (CDCl₃, 400 MHz) δ 10.06–10.77 (m, 1 H), 8.44 (d, $J = 8.0$

Hz, 1 H), 7.84 (d, $J = 8.0$ Hz, 1 H), 7.64 (d, $J = 8.8$ Hz, 1 H), 7.31 (d, $J = 8.8$ Hz, 1 H), 4.86 (d, $J = 3.9$ Hz, 1 H), 4.24 (s, 3 H), 3.10–3.42 (m, 2 H), 2.74–2.92 (m, 1 H), 2.61 (s, 3 H), 0.99 (d, $J = 7.0$ Hz, 3 H), 0.68 (d, $J = 6.8$ Hz, 3 H). ES-MS m/z 380.1 ($M + H$).

Step 6: (R)-6-(1-(5-Cyano-6-methylpyridin-2-yl)-5-isopropyl-4,5-dihydro-1H-pyrazol-3-yl)-2-methoxynicotinic Acid (**R-25**). This compound was obtained from racemic **25** using chiral HPLC (SFC conditions, Chiralpak AD-H, 10 mm \times 250 mm; mobile phase, 40/60 2-propanol/carbon dioxide; flow rate, 10 mL/min). Second eluting peak: chiral HPLC $t_R = 4.09$ min (Chiralpak AD-H, 40/60 2-propanol/carbon dioxide). 1H NMR (CH₃OH- d_4 , 400 MHz) δ 8.13 (d, $J = 7.81$ Hz, 1 H), 7.64 (dd, $J = 2.93, 8.39$ Hz, 2 H), 7.24 (d, $J = 8.59$ Hz, 1 H), 4.75–4.85 (m, 1 H), 3.97 (s, 3 H), 3.23–3.42 (m, 2 H), 2.73 (dt, $J = 3.71, 6.93$ Hz, 1 H), 2.48 (s, 3 H), 0.85–0.98 (d, $J = 7.02$ Hz, 3 H), 0.59 (d, $J = 7.02$ Hz, 3 H). ES-MS m/z 380.1 ($M + H$).

Synthesis of (R)-6-(1-(4-Cyano-3-methylphenyl)-5-cyclopentyl-4,5-dihydro-1H-pyrazol-3-yl)-2-methoxy-N-(methylsulfonyl)nicotinamide (R-26a). This compound was prepared from carboxylic acid **R-14c** (0.1 g, 0.247 mmol) and methanesulfonamide (0.036 g, 0.370 mmol) following general procedure D. **R-26a** was obtained as a yellow solid (0.035 g, 29%). 1H NMR (DMSO- d_6 , 500 MHz) δ 11.58 (s, 1 H), 8.05 (d, $J = 8.1$ Hz, 1 H), 7.74 (d, $J = 7.8$ Hz, 1 H), 7.61 (d, $J = 8.8$ Hz, 1 H), 7.27 (d, $J = 2.0$ Hz, 1 H), 7.16 (dd, $J = 8.5, 2.2$ Hz, 1 H), 4.92 (d, $J = 11.7$ Hz, 1 H), 4.02 (s, 3 H), 3.49 (dd, $J = 18.4, 11.6$ Hz, 1 H), 3.37 (s, 3 H), 3.22 (dd, $J = 18.5, 4.1$ Hz, 1 H), 2.53 (m, 1 H), 2.45 (s, 3 H), 1.72–1.84 (m, 1 H), 1.52 (m, 3 H), 1.21–1.45 (m, 3 H), 0.97–1.12 (m, 1 H). ES-MS m/z 482.1 ($M + H$). HPLC purity 99%, method 1.

Synthesis of (R)-6-(1-(5-Cyano-6-methylpyridin-2-yl)-5-cyclopentyl-4,5-dihydro-1H-pyrazol-3-yl)-2-methoxy-N-(methylsulfonyl)nicotinamide (R-26b). Carboxylic acid **R-14d** (0.08 g, 0.197 mmol), methanesulfonamide (0.019 g, 0.197 mmol), *N,N'*-diisopropylethylamine (0.137 mL, 0.788 mmol) and *N,N,N'*-tetramethyl-*O*-(7-azabenzotriazol-1-yl)uronium hexafluorophosphate (0.075 g, 0.197 mmol) were combined in dichloromethane (2 mL) and stirred at room temperature 16 h. The reaction was diluted with dichloromethane and extracted with water. The organic layer was washed with 0.1 N aqueous hydrochloric acid and brine, dried over magnesium sulfate, filtered, and concentrated. The residue was purified by column chromatography using a gradient of ethyl acetate in heptane (20–50%) to give **R-26b** as a yellow solid (0.045 g, 47%). 1H NMR (DMSO- d_6 , 500 MHz) δ 11.68 (br s, 1 H), 8.07 (d, $J = 7.8$ Hz, 1 H), 7.91 (d, $J = 9.0$ Hz, 1 H), 7.77 (d, $J = 7.8$ Hz, 1 H), 7.29 (d, $J = 8.8$ Hz, 1 H), 5.02 (dt, $J = 11.5, 4.6$ Hz, 1 H), 4.02 (s, 3 H), 3.52 (dd, $J = 18.7, 11.8$ Hz, 1 H), 3.37 (s, 3 H), 3.20 (dd, $J = 18.7, 4.5$ Hz, 1 H), 2.84 (d, $J = 5.1$ Hz, 1 H), 2.55 (s, 3 H), 1.67–1.77 (m, 1 H), 1.48–1.65 (m, 3 H), 1.28–1.46 (m, 3 H), 1.02–1.17 (m, 1 H). ES-MS m/z 483.0 ($M + H$). HPLC purity 97%, method 1.

Synthesis of (R)-6-(1-(4-Cyano-3-methylphenyl)-5-cyclopentyl-4,5-dihydro-1H-pyrazol-3-yl)-2-methoxy-N-(1H-tetrazol-5-yl)nicotinamide (R-27). This compound was prepared from carboxylic acid **R-14c** (0.09 g, 0.22 mmol) and 5-amino-tetrazole (0.028 g, 0.335 mmol) following general procedure D. **R-27** was obtained as a yellow solid (0.020 g, 19%). 1H NMR (DMSO- d_6 , 500 MHz) δ 11.57–12.10 (m, 1 H), 8.16 (d, $J = 7.8$ Hz, 1 H), 7.79 (d, $J = 7.8$ Hz, 1 H), 7.61 (d, $J = 8.5$ Hz, 1 H), 7.28 (d, $J = 2.0$ Hz, 1 H), 7.16 (dd, $J = 8.7, 2.3$ Hz, 1 H), 4.68–5.17 (m, 1 H), 4.06 (s, 3 H), 3.51 (d, $J = 6.3$ Hz, 1H), 3.27 (d, $J = 4.1$ Hz, 1 H), 2.53–2.60 (m, 1 H), 2.46 (s, 3 H), 1.71–1.85 (m, 1 H), 1.46–1.65 (m, 3 H), 1.23–1.45 (m, 3 H), 0.94–1.13 (m, 1 H). ES-MS m/z 472.1 ($M + H$). HPLC purity 99%, method 1.

All the biological assays including the functional and binding assay for the nuclear hormone receptors MR, PR, GR, AR, and ER α were performed as previously described.^{28,29}

Effect of (R)-14c on Urinary Sodium to Potassium Ratio (Na⁺/K⁺) in Sprague–Dawley Rats. All procedures were conducted in accordance with Institutional Animal Care and Use Committee guidelines and regulations at Pfizer Inc. (Groton, CT). Male, Sprague–Dawley rats were received from Charles River Laboratories at approximately 11 weeks of age (body weight = 300–400 g). Rats were singly housed in wire cages on a 12 h light cycle and were

provided standard laboratory chow diet and water ad libitum prior to and throughout the studies. Following acclimation, animals were randomly assigned to treatment groups ($n = 6/\text{group}$) to receive a single oral dose of 3, 10, or 30 mg/kg (R)-14c or vehicle (0.5% methylcellulose and 0.1% polysorbate 80) or 30 mg/kg eplerenone used as a positive control in a dosing volume of 5 mL/kg. Urine samples were collected overnight prior to dosing and at intervals of 0–2, 2–4, and 4–7 h postdose for measurement of urinary sodium and potassium concentration. Data were converted to $\text{Log}(10^* \text{Na}^+/\text{K}^+)$ and were analyzed using ANOVA with Dunnet's posthoc test. (R)-14c plasma concentration was measured using LC-MS.

Docking and MD Simulation. The docking experiment was carried out using GLIDE program.^{37–39} The protein structure was built based on the X-ray crystal structure of human mineralocorticoid receptor ligand-binding domain with a nonsteroidal antagonist at 1.34 Å resolution (PDB ID: 3VHV).³⁵ The original protein structure was prepared following the standard “Protein Preparation Wizard” in Maestro.⁴⁶ The initial 3D coordinates of ligand (R)-14c was first generated using LigPrep.⁴⁷ To remove the bias from the initial conformation, four different conformations of ligand (R)-14c were prepared using ConfGen.^{48,49} These four conformations were used as the initial input structures for the docking. The best binding pose from these four docking experiments was consistent. That pose was used for further optimization. After the initial binding pose generated, molecular dynamic simulation was used to optimize the protein–ligand interaction. The simulation was performed using Desmond program.^{50,51} The OPLS2005 force field^{52,53} was used to model all protein and ligand interactions, and the TIP3P water⁵⁴ was used as explicit solvent model. The details about the simulation setup have been described elsewhere.⁵⁵ A 1 ns NPT production simulation was then run and conformations were saved in 4.8 ps intervals. The structure with lowest potential energy was saved as the final binding mode.

AUTHOR INFORMATION

Corresponding Author

*Phone: 617-665-5673. E-mail: agustin.casimiro-garcia@pfizer.com.

Notes

The authors declare no competing financial interest.

ACKNOWLEDGMENTS

We thank Laurence Philippe and the Analytical Chemistry group for separation of several sets of enantiomers.

ABBREVIATIONS USED

AR, androgen receptor; BP, blood pressure; ER, estrogen receptor; GR, glucocorticoid receptor; MR, mineralocorticoid receptor; NHR, nuclear hormone receptor; PR, progesterone receptor; SDD, spray dried dispersion; UACR, urinary albumin to creatinine ratio

REFERENCES

- (1) Lu, N. Z.; Wardell, S. E.; Burnstein, K. L.; Defranco, D.; Fuller, P. J.; Giguere, V.; Hochberg, R. B.; McKay, L.; Renoir, J.-M.; Weigel, N. L.; Wilson, E. M.; McDonnell, D. P.; Cidlowski, J. A. International union of pharmacology. LXV. The pharmacology and classification of the nuclear receptor superfamily: glucocorticoid, mineralocorticoid, progesterone, and androgen receptors. *Pharmacol. Rev.* **2006**, *58*, 782–797.
- (2) Moore, J. T.; Collins, J. L.; Pearce, K. H. Nuclear receptor superfamily and drug discovery. *ChemMedChem* **2006**, *1*, 504–523.
- (3) Catena, C.; Colussi, G.; Marzano, L.; Sechi, L. A. Aldosterone and the heart: from basic research to clinical evidence. *Horm. Metab. Res.* **2012**, *44*, 181–187.

- (4) Fourkietis, V. G.; Hanslik, G.; Hanusch, F.; Lepenies, J.; Quinkler, M. Aldosterone and the kidney. *Horm. Metab. Res.* **2012**, *44*, 194–201.

- (5) Lam, E. Y. M.; Funder, J. W.; Nikolic-Paterson, D. J.; Fuller, P. J.; Young, M. J. Mineralocorticoid receptor blockade but not steroid withdrawal reverses renal fibrosis in deoxycorticosterone/salt rats. *Endocrinology* **2006**, *147*, 3623–3629.

- (6) Lieber, G. B.; Fernandez, X.; Mingo, G. G.; Jia, Y.; Caniga, M.; Gil, M. A.; Keshwani, S.; Woodhouse, J. D.; Cicmil, M.; Moy, L. Y.; Kelly, N.; Jimenez, J.; Crawley, Y.; Anthes, J. C.; Klappenbach, J.; Ma, Y.-L.; McLeod, R. L. Mineralocorticoid receptor antagonists attenuate pulmonary inflammation and bleomycin-evoked fibrosis in rodent models. *Eur. J. Pharmacol.* **2013**, *718*, 290–298.

- (7) Hu, Q.; Yin, L.; Hartmann, R. W. Aldosterone synthase inhibitors as promising treatments for mineralocorticoid dependent cardiovascular and renal diseases. *J. Med. Chem.* **2014**, DOI: dx.doi.org/10.1021/jm401430e.

- (8) Pitt, B.; Zannad, F.; Remme, W. J.; Cody, R.; Castaigne, A.; Perez, A.; Palensky, J.; Wittes, J. The effect of spironolactone on morbidity and mortality in patients with severe heart failure. *N. Engl. J. Med.* **1999**, *341*, 709–717.

- (9) Pitt, B.; Remme, W.; Zannad, F.; Neaton, J.; Martinez, F.; Roniker, B.; Bittman, R.; Hurley, S.; Kleiman, J.; Gatlin, M. Eplerenone, a selective aldosterone blocker, in patients with left ventricular dysfunction after myocardial infarction. *N. Engl. J. Med.* **2003**, *348*, 1309–1321.

- (10) Zannad, F.; McMurray, J. J. V.; Krum, H.; van, V. D. J.; Swedberg, K.; Shi, H.; Vincent, J.; Pocock, S. J.; Pitt, B. Eplerenone in patients with systolic heart failure and mild symptoms. *N. Engl. J. Med.* **2011**, *364*, 11–21.

- (11) Rossing, K.; Schjoedt, K. J.; Smidt, U. M.; Boomsma, F.; Parving, H.-H. Beneficial effects of adding spironolactone to recommended antihypertensive treatment in diabetic nephropathy: a randomized, double-masked, cross-over study. *Diabetes Care* **2005**, *28*, 2106–2112.

- (12) van, d. M. A. H.; Baggen, R. G.; Pauli, S.; Lindemans, A.; Vulto, A. G.; Poldermans, D.; Boomsma, F. Spironolactone in type 2 diabetic nephropathy: effects on proteinuria, blood pressure and renal function. *J. Hypertens.* **2006**, *24*, 2285–2292.

- (13) Nielsen, S. E.; Persson, F.; Frandsen, E.; Sugaya, T.; Hess, G.; Zdunek, D.; Shjoedt, K. J.; Parving, H. H.; Rossing, P. Spironolactone diminishes urinary albumin excretion in patients with type 1 diabetes and microalbuminuria: a randomized placebo-controlled crossover study. *Diabetic Med.* **2012**, *29*, e184–e190.

- (14) Esteghamati, A.; Noshad, S.; Jarrah, S.; Mousavizadeh, M.; Khoei, S. H.; Nakhjavani, M. Long-term effects of addition of mineralocorticoid receptor antagonist to angiotensin II receptor blocker in patients with diabetic nephropathy: a randomized clinical trial. *Nephrol., Dial., Transplant.* **2013**, *28*, 2823–2833.

- (15) McManus, F.; McInnes, G. T.; Connell, J. M. C. Drug Insight: eplerenone, a mineralocorticoid-receptor antagonist. *Nature Clin. Pract. Endocrinol. Metab.* **2008**, *4*, 44–52.

- (16) Roscioni, S. S.; de, Z. D.; Bakker, S. J. L.; Lambers, H. H. J. Management of hyperkalaemia consequent to mineralocorticoid-receptor antagonist therapy. *Nature Rev. Nephrol.* **2012**, *8*, 691–699.

- (17) Piotrowski, D. W. Mineralocorticoid receptor antagonists for the treatment of hypertension and diabetic nephropathy. *J. Med. Chem.* **2012**, *55*, 7957–7966.

- (18) Baerfacker, L.; Kuhl, A.; Hillisch, A.; Grosser, R.; Figueroa-Perez, S.; Heckroth, H.; Nitsche, A.; Ergueden, J.-K.; Gielen-Haertwig, H.; Schlemmer, K.-H.; Mittendorf, J.; Paulsen, H.; Platzeck, J.; Kolkhof, P. Discovery of BAY 94-8862: a nonsteroidal antagonist of the mineralocorticoid receptor for the treatment of cardiorenal diseases. *ChemMedChem* **2012**, *7*, 1385–1403.

- (19) Pitt, B.; Kober, L.; Ponikowski, P.; Gheorghiad, M.; Filippatos, G.; Krum, H.; Nowack, C.; Kolkhof, P.; Kim, S.-Y.; Zannad, F. Safety and tolerability of the novel non-steroidal mineralocorticoid receptor antagonist BAY 94-8862 in patients with chronic heart failure and mild

or moderate chronic kidney disease: a randomized, double-blind trial. *Eur. Heart J.* **2013**, *34*, 2453–2463.

(20) Platt, D.; Pauli, H. Studies on organ- and subcellular distribution of 3H-spirolactone in animals. *Arzneim. Forsch.* **1972**, *22*, 1801–1802.

(21) Kolkhof, P.; Borden, S. A. Molecular pharmacology of the mineralocorticoid receptor: prospects for novel therapeutics. *Mol. Cell. Endocrinol.* **2012**, *350*, 310–317.

(22) Meyers, M. J.; Arhancet, G. B.; Chen, X.; Hockerman, S. L.; Long, S. A.; Mahoney, M. W.; Reitz, D. B.; Rico, J. G. Preparation of tetrahydro-2H-benzo[g]indazole compounds as mineralocorticoid receptor antagonists. WO2008053300A1, 2008.

(23) Dietz, J. D.; Du, S.; Bolten, C. W.; Payne, M. A.; Xia, C.; Blinn, J. R.; Funder, J. W.; Hu, X. A number of marketed dihydropyridine calcium channel blockers have mineralocorticoid receptor antagonist activity. *Hypertension* **2008**, *51*, 742–748.

(24) Arhancet, G. B.; Woodard, S. S.; Dietz, J. D.; Garland, D. J.; Wagner, G. M.; Iyanar, K.; Collins, J. T.; Blinn, J. R.; Numann, R. E.; Hu, X.; Huang, H.-C. Stereochemical requirements for the mineralocorticoid receptor antagonist activity of dihydropyridines. *J. Med. Chem.* **2010**, *53*, 4300–4304.

(25) Arhancet, G. B.; Woodard, S. S.; Iyanar, K.; Case, B. L.; Woerndle, R.; Dietz, J. D.; Garland, D. J.; Collins, J. T.; Payne, M. A.; Blinn, J. R.; Pomposiello, S. I.; Hu, X.; Heron, M. I.; Huang, H.-C.; Lee, L. F. Discovery of novel cyanodihydropyridines as potent mineralocorticoid receptor antagonists. *J. Med. Chem.* **2010**, *53*, 5970–5978.

(26) Arhancet, G. B.; Casimiro-Garcia, A.; Chen, X.; Hepworth, D.; Meyers, M. J.; Piotrowski, D. W.; Raheja, R. K. Preparation of 4,5-dihydro-1H-pyrazole compounds as mineralocorticoid receptor antagonists. WO2010116282A1, 2010.

(27) Casimiro-Garcia, A.; Futatsugi, K.; Piotrowski, D. W. Preparation of morpholine compounds as therapeutic mineralocorticoid receptor antagonists. WO2011141848A1, 2011.

(28) Futatsugi, K.; Piotrowski, D. W.; Casimiro-Garcia, A.; Robinson, S.; Sammons, M.; Loria, P. M.; Banker, M. E.; Petersen, D. N.; Schmidt, N. J. Design and synthesis of aryl sulfonamide-based nonsteroidal mineralocorticoid receptor antagonists. *Bioorg. Med. Chem. Lett.* **2013**, *23*, 6239–6242.

(29) Meyers, M. J.; Arhancet, G. B.; Hockerman, S. L.; Chen, X.; Long, S. A.; Mahoney, M. W.; Rico, J. R.; Garland, D. J.; Blinn, J. R.; Collins, J. T.; Yang, S.; Huang, H.-C.; McGee, K. F.; Wendling, J. M.; Dietz, J. D.; Payne, M. A.; Homer, B. L.; Heron, M. I.; Reitz, D. B.; Hu, X. Discovery of (3S,3aR)-2-(3-chloro-4-cyanophenyl)-3-cyclopentyl-3,3a,4,5-tetrahydro-2H-benzo[g]indazole-7-carboxylic acid (PF-3882845), an orally efficacious mineralocorticoid receptor (MR) antagonist for hypertension and nephropathy. *J. Med. Chem.* **2010**, *53*, 5979–6002.

(30) Compound 2, also known as PF-03882845, is now commercially available from Sigma Aldrich (catalogue no. PZ0031).

(31) Orena, S.; Maurer, T. S.; She, L.; Eudy, R.; Bernardo, V.; Dash, D.; Loria, P.; Banker, M. E.; Tugnait, M.; Okerberg, C. V.; Qian, J.; Boustany-Kari, C. M. PF-03882845, a non-steroidal mineralocorticoid receptor antagonist, prevents renal injury with reduced risk of hyperkalemia in an animal model of nephropathy. *Front. Pharmacol.* **2013**, *4*, 115.

(32) PF-03882845 was dosed as 75% spray dried dispersion (SDD) in Phase 1 clinical trial. See *A Study Of PF-03882845 Absorption In Healthy Volunteers Given Orally As Tablet Versus Suspension Formulations And Effect Of Food On Its Absorption*; U.S. National Library of Medicine: Bethesda, MD, 2011; <http://clinicaltrials.gov/show/NCT01366287>.

(33) Boos, C.; Bowles, D. M.; Cai, C.; Casimiro-Garcia, A.; Chen, X.; Hulford, C. A.; Jennings, S. M.; Kiser, E. J.; Piotrowski, D. W.; Sammons, M.; Wade, R. A. Synthesis and cross coupling of a highly substituted 2-pyridylboronate: application to the large scale synthesis of a mineralocorticoid antagonist. *Tetrahedron Lett.* **2011**, *52*, 7025–7029.

(34) Dehring, K. A.; Workman, H. L.; Miller, K. D.; Mandagere, A.; Poole, S. K. Automated robotic liquid handling/laser-based nephelometry system for high throughput measurement of kinetic aqueous solubility. *J. Pharm. Biomed. Anal.* **2004**, *36*, 447–456.

(35) Hasui, T.; Matsunaga, N.; Ora, T.; Ohyabu, N.; Nishigaki, N.; Imura, Y.; Igata, Y.; Matsui, H.; Motoyaji, T.; Tanaka, T.; Habuka, N.; Sogabe, S.; Ono, M.; Siedem, C. S.; Tang, T. P.; Gauthier, C.; De, M. L. A.; Boyd, S. A.; Fukumoto, S. Identification of benzoxazin-3-one derivatives as novel, potent, and selective nonsteroidal mineralocorticoid receptor antagonists. *J. Med. Chem.* **2011**, *54*, 8616–8631.

(36) Hasui, T.; Ohra, T.; Ohyabu, N.; Asano, K.; Matsui, H.; Mizukami, A.; Habuka, N.; Sogabe, S.; Endo, S.; Siedem, C. S.; Tang, T. P.; Gauthier, C.; De, M. L. A.; Boyd, S. A.; Fukumoto, S. Design, synthesis, and structure–activity relationships of dihydrofuran-2-one and dihydropyrrol-2-one derivatives as novel benzoxazin-3-one-based mineralocorticoid receptor antagonists. *Bioorg. Med. Chem.* **2013**, *21*, 5983–5994.

(37) Friesner, R. A.; Banks, J. L.; Murphy, R. B.; Halgren, T. A.; Klicic, J. J.; Mainz, D. T.; Repasky, M. P.; Knoll, E. H.; Shelley, M.; Perry, J. K.; Shaw, D. E.; Francis, P.; Shenkin, P. S. Glide: A new approach for rapid, accurate docking and scoring. 1. Method and assessment of docking accuracy. *J. Med. Chem.* **2004**, *47*, 1739–1749.

(38) Halgren, T. A.; Murphy, R. B.; Friesner, R. A.; Beard, H. S.; Frye, L. L.; Pollard, W. T.; Banks, J. L. Glide: A new approach for rapid, accurate docking and scoring. 2. Enrichment factors in database screening. *J. Med. Chem.* **2004**, *47*, 1750–1759.

(39) *Small-molecule drug discovery suite 2013-3: Glide*, version 6.1; Schrödinger, LLC: New York, 2013.

(40) Fagart, J.; Huyet, J.; Pinon, G. M.; Rochel, M.; Mayer, C.; Rafestin-Oblin, M.-E. Crystal structure of a mutant mineralocorticoid receptor responsible for hypertension. *Nature Struct. Mol. Biol.* **2005**, *12*, 554–555.

(41) Li, Y.; Suino, K.; Daugherty, J.; Xu, H. E. Structural and biochemical mechanisms for the specificity of hormone binding and coactivator assembly by mineralocorticoid receptor. *Mol. Cell* **2005**, *19*, 367–380.

(42) Bledsoe, R. K.; Madauss, K. P.; Holt, J. A.; Apolito, C. J.; Lambert, M. H.; Pearce, K. H.; Stanley, T. B.; Stewart, E. L.; Trump, R. P.; Willson, T. M.; Williams, S. P. A Ligand-mediated hydrogen bond network required for the activation of the mineralocorticoid receptor. *J. Biol. Chem.* **2005**, *280*, 31283–31293.

(43) Huyet, J.; Pinon, G. M.; Fay, M. R.; Fagart, J.; Rafestin-Oblin, M.-E. Structural basis of spiroactone recognition by the mineralocorticoid receptor. *Mol. Pharmacol.* **2007**, *72*, 563–571.

(44) Eudy, R. J.; Sahasrabudhe, V.; Sweeney, K.; Tugnait, M.; King-Ahmad, A.; Near, K.; Loria, P.; Banker, M. E.; Piotrowski, D. W.; Boustany-Kari, C. M. The use of plasma aldosterone and urinary sodium to potassium ratio as translatable quantitative biomarkers of mineralocorticoid receptor antagonism. *J. Transl. Med.* **2011**, *9*, 180.

(45) Sanchez, J. P. An efficient synthesis and mechanism of formation of 6-acetyl-1,2-dihydro-2-oxo-3-pyridinecarboxylic acid. *Tetrahedron* **1990**, *46*, 7693–7698.

(46) *Schrödinger Release 2013-3: Maestro*, version 9.6; Schrödinger, LLC: New York, 2013.

(47) *Schrödinger Release 2013-3: LigPrep*, version 2.8; Schrödinger, LLC: New York, 2013.

(48) Watts, K. S.; Dalal, P.; Murphy, R. B.; Sherman, W.; Friesner, R. A.; Shelley, J. C. ConfGen: a conformational search method for efficient generation of bioactive conformers. *J. Chem. Inf. Model.* **2010**, *50*, 534–546.

(49) *Schrödinger Release 2013-3: ConfGen*, version 2.6; Schrödinger, LLC: New York, 2013.

(50) *Schrödinger Release 2013-3: Desmond Molecular Dynamics System*, version 3.6; D. E. Shaw Research: New York, 2013.

(51) *Maestro–Desmond Interoperability Tools*, version 3.6; Schrödinger, LLC: New York, 2013.

(52) Jorgensen, W. L.; Maxwell, D. S.; Tirado-Rives, J. Development and testing of the OPLS all-atom force field on conformational

energetics and properties of organic liquids. *J. Am. Chem. Soc.* **1996**, *118*, 11225–11236.

(53) Kaminski, G. A.; Friesner, R. A.; Tirado-Rives, J.; Jorgensen, W. L. Evaluation and reparametrization of the OPLS-AA force field for proteins via comparison with accurate quantum chemical calculations on peptides. *J. Phys. Chem. B* **2001**, *105*, 6474–6487.

(54) Jorgensen, W. L.; Chandrasekhar, J.; Madura, J. D.; Impey, R. W.; Klein, M. L. Comparison of simple potential functions for simulating liquid water. *J. Chem. Phys.* **1983**, *79*, 926–935.

(55) Guo, Z.; Mohanty, U.; Noehre, J.; Sawyer, T. K.; Sherman, W.; Krilov, G. Probing the α -helical structural stability of stapled p53 peptides: molecular dynamics simulations and analysis. *Chem. Biol. Drug Des.* **2010**, *75*, 348–359.